Nitrogen-Rich Tetrazolium Azotetrazolate Salts: A New Family of Insensitive Energetic Materials

Thomas M. Klapötke* and Carles Miró Sabaté

Energetic Materials Research, Department of Chemistry and Biochemistry, Ludwig-Maximilian University of Munich, Butenandstrasse 5-13 (D), 81377 Munich, Germany

Received November 24, 2007. Revised Manuscript Received December 19, 2007

The metathesis reaction of sodium azotetrazolate with tetrazolium iodides **5**and **6** at reflux in water yielded dihydrated species in both instances (**1** and **3**, respectively). However, when silver azotetrazolate (Ag_2ZT) was used instead of the sodium salt in dry methanol, the anhydrous compounds **2** and **4** formed. An alternative synthesis for **2** and **4** that avoids handling highly sensitive Ag_2ZT is introduced. All materials were fully characterized by means of elemental analysis, mass spectrometry (MS), and vibrational (IR, Raman) and NMR (^1H, ^{13}C) spectroscopy. Additionally, the crystal structures of the new compounds were determined (**1**, monoclinic, $P2_1/c$; **2–4**, triclinic,$P\bar{1}$). A discussion of the hydrogen bonding by means of graph-set analysis is provided. The thermal behaviors of **1–4** and their constant volume energies of combustion were assessed by DSC and bomb calorimetry measurements, respectively. Their sensitivity to shock, friction, and electrostatic discharge was measured by submitting the compounds to standard tests. The detonation pressures and velocities were calculated from the energies of formation using the EXPLO5 code (**1**, $P = 20.2$ GPa, $D = 7820$ m s^{-1}; **2**, $P = 20.0$ GPa, $D = 7803$ m s^{-1}; **3**, $P = 22.4$ GPa, $D = 8090$ m s^{-1}; and **4**, $P = 21.1$ GPa, $D = 7977$ m s^{-1}. Lastly, the decomposition products were both calculated and experimentally determined.

Introduction

There has been considerable interest in high-energy density materials (HEDMs) in recent years.[1–9] Some of the most promising developments in the chemistry of HEDMs are compounds that combine a high nitrogen content (because the majority of the decomposition products will be molecular N_2) with a high heat of formation and insensitivity to shock, friction, and electrostatic discharge.[10,11]

5,5′-Azotetrazole (H_2ZT) is an azo compound with an extremely high nitrogen content (84.3%), making it of interest for the synthesis of highly energetic materials if it were more chemically stable. The compound was described by Thiele[12] more than a century ago to readily decompose at room temperature, evolving nitrogen to yield 5-hydrazino-*1H*-tetrazole and formic acid. The instability of H_2ZT was confirmed in our group[13] and 5,5′-azotetrazole was shown to be stable only at temperatures below −30 °C in methanol solution as a methanol adduct in the solid state, as shown by crystal structure determination.

* To whom correspondence should be addressed. Fax: (49) 89-2180-77492. E-mail: tmk@cup.uni-muenchen.de.

(1) (a) Adam, D.; Holl, G.; Klapötke, T. M. *Heteroat. Chem.* **1999**, *10* (7), 548–553. (b) Klapötke, T. M.; Ang, H.-G. *Propellants, Explos., Pyrotech.* **2001**, *26* (5), 221–224. (c) Hammerl, A.; Klapötke, T. M.; Nöth, H.; Warchhold, M.; Holl, G.; Kaiser, M.; Ticmanis, U. *Inorg. Chem.* **2001**, *40* (14), 3570–3575. (d) Klapötke, T. M.; Mayer, P.; Schulz, A.; Weigand, J. J. *Propellants, Explos., Pyrotech.* **2004**, *29* (6), 325–332. (e) Klapötke, T. M.; Holl, G.; Geith, J.; Hammerl, A.; Weigand, J. *Proceedings of the 7th Seminar on New Trends in the Research of Energetic Materials*, Pardubice, Czech Republic, April 20–22, 2004; Institute of Energetic Materials, University of Pardubice: Pardubice, Czech Republic, 2004. (f) Clark, K. A.; Klapötke, T. M. *230th ACS National Meeting*, Washington, DC, United States, Aug 28−Sept 1, 2005: American Chemical Society: Washington, D.C., 2005.

(2) (a) Göbel, M.; Karaghiosoff, K.; Klapötke, T. M.; Miró-Sabaté, C.; Welch, J. M. *Proceedings of the 9th Seminar on New Trends in the Research of Energetic Materials*, Pardubice, Czech Republic, April 19–21, 2006; Institute of Energetic Materials, University of Pardubice: Pardubice, Czech Republic, 2006. (b) Klapötke, T. M.; Mayer, P.; Miró-Sabaté, C.; Penger, A.; Welch, J. M. 233rd ACS National Meeting, Chicago, IL, United States, 25–29 March, 2007. (c) Klapötke, T. M.; Miró-Sabaté, C. *Proceedings of the 10th Seminar on New Trends in the Research of Energetic Materials*, Pardubice, Czech Republic, April 25−27, 2007; Institute of Energetic Materials, University of Pardubice: Pardubice, Czech Republic, 2007.

(3) (a) Oestmark, H. *Proceedings of the 9th Seminar on New Trends in the Research of Energetic Materials*, Pardubice, Czech Republic, April 19–21, 2006; Institute of Energetic Materials, University of Pardubice: Pardubice, Czech Republic, 2006. (b) Oestmark, H.; Walin, S.; Goede, P. *Cent. Eur. J. Energ. Mater.* **2007**, *4* (1–2), 83–108.

(4) (a) Bruney, L. Y.; Bledson, T. M.; Strout, D. L. *Inorg. Chem.* **2003**, *42* (24), 8117–8120. (b) Strout, D. L. *J. Phys. Chem. A* **2004**, *108* (49), 10911–10916.

(5) (a) Qiu, L.; Xiao, H.-M. *Hanneng Cailiao* **2006**, *14* (2), 158. (b) Rosi, M.; de Petris, G.; Troiani, A. *Abstracts of Papers from the 232nd ACS National Meeting*,San Francisco, CA, Sept 10–14, 2006; American Chemical Society: Washington, D.C., 2006.

(6) Steinhauser, G.; Crawford, M.-J.; Darwich, C.; Klapötke, T. M.; Miró-Sabaté, C.; Welch, J. M. *Acta Crystallogr., Sect. E* **2007**, *63*, o3100–o3101.

(7) Uddin, J.; Barone, V.; Scuseria, G. E. *Mol. Phys.* **2006**, *104* (5–7), 745–749.

(8) Nguyen, M. T. *Coord. Chem. Rev.* **2003**, *244* (1–2), 93–113.

(9) Ding, Y.-H.; Inagaki, S. *Chem. Lett.* **2003**, *32* (3), 304–305.

(10) Borne, L.; Herrmann, M.; Skidmore, C. B. *Microstructure and Morphology in Energetic Materials–Particle Processing and Characterization*; Wiley−VCH: Weinheim, Germany, 2005, 333–366.

(11) Klapötke, T. M.; Miró-Sabaté, C. *Insensitive Energetic Materials. Particles, Crystals, Composites ICT Symposium*,Pfinztal, Germany, March 13–14, 2007; Fraunhofer IRB Verlag: Stuttgart, Germany, 2007.

(12) (a) Thiele, J. *Just. Lieb. Ann. Chem.* **1892**, *270*, 54–63. (b) Thiele, J.; Marais, J. T. *Just. Lieb. Ann. Chem.* **1893**, *273*, 144–160. (c) Thiele, J. *Ber. Dtsch. Chem. Ges.* **1893**, *26*, 2645–2646. (d) Thiele, J. *Just. Lieb. Ann. Chem.* **1898**, *303*, 57–75.

10.1021/cm703344h CCC: $40.75 © 2008 American Chemical Society
Published on Web 02/15/2008

Because of its high nitrogen content, high heat of formation (due mainly to nitrogen catenation), and ready availability, there has been increasing recent interest in the synthesis of energetic salts based on the azotetrazolate anion. The cations of choice thus far have been those of easily protonated nitrogen bases such as ammonium,[14] hydrazinium,[1c] guanidinium, aminoguanidinium, diaminoguanidinium, or triaminoguanidinium,[15] giving rise to compounds with a high nitrogen content ranging from 78.8% for the bisguanidinium salt to 85.2% for the bishydrazinium derivative. Bishydrazinium 5,5′-azotetrazolate dihydrazinate[1c] was successfully synthesized in our research group and with a nitrogen content of 85.7% counts as the nitrogen-richest stable CHN compound known to date.

Thiele[12d] described the first synthesis of disodium azotetrazolate pentahydrate (among other metal salts), which Klapötke et al.[13] metathesized with a wide variety of metal salts yielding a whole family of metal azotetrazolate salts (Li, K, Rb, Cs, Mg, Ca, Sr, Ba, Al, Y, La, Ce, Nd, and Gd). All of these salts include varying numbers of crystal water incorporated into the solid state structure. The disodium salt (Na_2ZT) is the most readily accessible azotetrazolate described in the literature and can be synthesized by oxidizing 5-amino-*1H*-tetrazole (5-at) with potassium permanganate in sodium hydroxide solution (eq).[12d]

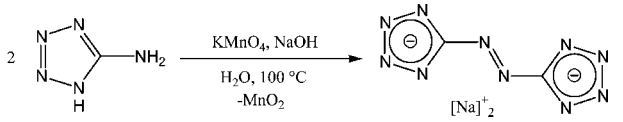

(1)

Many 5,5′-azotetrazolate salts have found practical application: several salts with nitrogen bases (e.g., guanidinium, triaminoguanidinium, and hydrazinium) have been used in gas generators for airbags as well as in fire extinguishing systems,[1c,14] heavy metal salts of 5,5′-azotetrazolate (e.g., $[Pb(OH)]^+$) have been used as initiators,[16] 1,1′-dimethyl-5–5′-azotetrazole has been used as an additive in solid rocket propellants,[17] etc.

Excluding this work, there are only three tetrazolium azotetrazolates described in the literature so far. 1,4,5-Trimethyltetrazolium azotetrazolate synthesized by Shreeve et al.[18] has a high positive heat of formation of +1547 kJ kg^{-1}. The nitrogen-richer 5-amino-*1H*-tetrazolium and 1,5-diaminotetrazolium azotetrazolate were also claimed to have been synthesized by Tremblay and co-workers[19] by metathesis of potassium azotetrazolate with the corresponding tetrazolium chloride in water. However, repetition of these syntheses by the literature procedure failed. Gas evolution followed by decoloration of the yellow solution was observed.

Recently, we have reported the synthesis of hydrazinebistetrazole (HBT), which is formally the product of reduction of the azo-bridge in the highly labile 5,5′-azotetrazole free acid, and proved it to be a very stable nitrogen-rich energetic compound with a high crystal density ($\rho = 1.841$ g cm^{-3}) that was used as a starting material for an alternative safer synthesis of 5,5′-azotetrazolate salts.[20] In this context, we intended to synthesize new examples of tetrazolium azotetrazolates in order to generate new compounds that may have interesting properties, including the aforementioned high nitrogen content, high heat of formation, and low sensitivity to classical stimuli (shock, friction, and electrostatic discharge). We also hope to eventually, in further studies, combine such compounds with an oxidizer such as ammonium nitrate (AN) or ammonium dinitramide (ADN) in order to investigate the suitability of such mixtures as high explosives/propellants and assess their performance as well as those of the mixtures.

Experimental Section

Caution! *Although no problems occurred during the synthesis and handling of the materials studied in this work, silver azotetrazolate, aminotetrazoles, and their derivatives are energetic materials and tend to explode under certain conditions. All HEDMs should be treated with respect and appropriate safety precautions should be taken at all times. Laboratories and personnel should be properly grounded and safety equipment such as Kevlar gloves, leather coat, face shield, and ear plugs are necessary, in particular when working on a larger scale.*

General Method. All chemicals and solvents (analytical grade) were used as supplied by Sigma-Aldrich Inc. Disodium 5,5′-azotetrazolate pentahydrate[12d] and 1,4-dimethyl-5-aminotetrazolium (**5**)[21] and 1,5-diamino-4-methyltetrazolium (**6**)[22] iodides were synthesized according to known procedures. ^1H and ^{13}C NMR spectra were recorded on a JEOL Eclipse 400 instrument in DMSO-d_6 at or near 25 °C. The chemical shifts are given relative to tetramethylsilane as external standard. Infrared (IR) spectra were recorded on a Perkin-Elmer Spectrum One FT-IR instrument as KBr pellets at 20 °C. Transmittance values are qualitatively described as "very strong" (vs), "strong" (s), "medium" (m), and "weak" (w). Raman spectra were recorded on a Perkin-Elmer Spectrum 2000R NIR FT-Raman instrument equipped with a Nd:YAG laser (1064 nm). The intensities are reported as percentages of the most intense peak and are given in parentheses. Elemental analyses were performed with a Netsch Simultanous Thermal

(13) (a) Hammerl, A.; Holl, G.; Klapötke, T. M.; Mayer, P.; Nöth, H.; Piotrowski, H.; Warchhold, M. *Eur. J. Inorg. Chem.* **2002**, *4*, 834–845. (b) Hammerl, A. Ph. D. Thesis, Ludwig-Maximilans Universität München, Munich, Germany, 2001.
(14) Hiskey, M. A.; Goldman, N.; Stine, J. R. *J. Energ. Mater.* **1998**, *16* (2 & 3), 119–127.
(15) Hammerl, A.; Hiskey, M. A.; Holl, G.; Klapötke, T. M.; Polborn, K.; Stierstorfer, J.; Weigand, J. J. *Chem. Mater.* **2005**, *17* (14), 3784–3793.
(16) (a) Chaudhri, M. M. *Nature* **1976**, *263*, 121–122. (b) Reddy, G. O.; Chatterjee, A. K. *Nature* **1983**, *66*, 231–244. (c) Whelan, D. J.; Spear, R. J.; Read, R. W. *Thermochim. Acta,* **1984**, *80*, 149–163. (d) Chaudhri, M. M. *J. Mater. Sci. Lett.* **1984**, *3*, 565–568.
(17) (a) Williams, M. M.; McEwan, W. S.; Henry, R. A. *J. Phys. Chem.* **1957**, *61*, 261–267. (b) Pan, W. *24th International Annual Conference of the ICT*, 1994, 77.
(18) (a) Ye, C.; Xiao, J.-C.; Twamley, B.; Shreeve, J. M. *Chem. Commun.* **2005**, *21*, 2750–2752. (b) Gao, H.; Ye, C.; Piekarski, C. M.; Shreeve, J. M. *J. Phys. Chem. A* **2007**, *111* (28), 10718–10731.
(19) Tremblay, M. *Can. J. Chem.* **1965**, *43* (5), 1154–1157.
(20) Klapötke, T. M.; Miró-Sabaté, C. *Z. Anorg. Allg. Chem.* **2007**, *633*, 2671–2677.
(21) Klapötke, T. M.; Karaghiosoff, K.; Mayer, P.; Penger, A.; Welch, J. M. *Propellants, Explos., Pyrotech.* **2006**, *31* (3), 188–195.
(22) (a) Gálvez-Ruiz, J. C.; Holl, G.; Karaghiosoff, K.; Klapötke, T. M.; Loehnwitz, K.; Mayer, P.; Nöth, H.; Polborn, K.; Rohbogner, C. J.; Suter, M.; Weigand, J. J. *Inorg. Chem.* **2005**, *44* (12), 4237–4253. (b) Gálvez-Ruiz, J. C.; Holl, G.; Karaghiosoff, K.; Klapötke, T. M.; Loehnwitz, K.; Mayer, P.; Nöth, H.; Polborn, K.; Rohbogner, C. J.; Suter, M.; Weigand, J. J. *Inorg. Chem.* **2005**, *44* (12), 5192–5192 Correction.

Analyzer STA 429. Melting points were determined by differential scanning calorimetry (Linseis DSC PT-10 instrument,[23] calibrated with standard pure indium and zinc). Measurements were performed at a heating rate of 5 °C min^{-1} in closed aluminum sample pans with a 1 μm hole in the top for gas release under a nitrogen flow of 20 mL min^{-1} with an empty identical aluminum sample pan as a reference.

Explosion Experiments. For the analysis of the explosion gases of all compounds, a steel bomb (dried at 100 °C for several days) with a volume of 100 mL was loaded with the corresponding salt (~100 mg). One end of the bomb was sealed and the other end was attached to a valve for gas transfer after the explosion had occurred. The bomb was evacuated with a vacuum line (~1×10^{-3} mbar) and the valve was closed. The explosion and/or decomposition was induced by placing the compound in the bottom of the bomb and heating it directly for 5–10 min with a Bunsen burner. The explosion products were allowed to expand in the bomb and after cooling the apparatus was attached to a mass spectrometer (JEOL MStation JMS 700).[24] The reservoir of the spectrometer was evacuated during 15 min prior to opening the valve in the bomb and allowing the decomposition gases to diffuse into the ionization source. The explosion gases were then analyzed by mass spectrometry using electron impact (EI) mode (mass range 1–120, 1 scan per second). The same bomb was attached to a previously evacuated IR gas cell (NaCl windows) and the gases were left to slowly diffuse into the cell by shortly opening the valve. The evacuated IR cell was measured as the background and subsequently the IR spectrum of the sample was recorded (5 scans, 4000−450 cm^{-1}, resolution = 4.0) on a Perkin-Elmer Spektrum One FT-IR instrument.[25]

Bomb Calorimetry. For all calorimetric measurements, a Parr 1356 bomb calorimeter (static jacket) equipped with a Parr 207A oxygen bomb for the combustion of highly energetic materials was used.[26] A Parr 1755 printer, furnished with the Parr 1356 calorimeter, was used to produce a permanent record of all activities within the calorimeter. The samples (~200 mg each) were carefully mixed with ~800 mg analytical grade benzoic acid and pressed into pellets, which were subsequently burned in a 3.05 MPa atmosphere of pure oxygen. The experimentally determined constant volume energies of combustion were obtained as the averages of three single measurements. The calorimeter was calibrated by the combustion of certified benzoic acid in an oxygen atmosphere at a pressure of 3.05 MPa.

Synthesis of 1,4-Dimethyl-5-aminotetrazolium Azotetrazolate Dihydrate (1). Sodium azotetrazolate pentahydrate (5.003 g, 16.7 mmol) was dissolved in 50 mL of hot water, yielding a clear bright yellow solution, and 1,4-dimethyl-5-aminotetrazolium iodide (8.076 g, 33.5 mmol) was added neat in small portions. The reaction mixture was boiled for 1 h before the oil bath and stirring were switched off. Immediate precipitation of the product was observed as the reaction mixture cooled. The resulting solution was stored in a refrigerator for 2 h. After this time, the yellow powder was filtered and recrystallized from a minimal amount of hot water. After cooling in a refrigerator for 2 h longer, the precipitated solid was filtered and washed with 10 mL of cold water, 30 mL of acetone, and 30 mL of ether. Lastly, the product was left to air-dry (5.491 g, 79%). Several crystals of the product suitable for X-ray structure analysis could be obtained together with powdery bulk material when the same reaction was conducted in a 1 mmol scale and the mother liquors were kept in the fridge for 1 week. $C_8H_{20}N_{20}O_2$ (calcd/found): C 22.42/22.49, H 4.71/4.60, N 65.40/65.68. DSC (5 °C min^{-1}, °C): 84 (-H_2O), 197 (mp + dec.). *m/z* (FAB^+, xenon, 6 keV, m-NBA matrix): 114.2 $[DMAT]^+$; *m/z* (FAB^-, xenon, 6 keV, m-NBA matrix): 165.2 $[C_2N_{10}H]^-$. ^{1}H NMR (DMSO-d_6, 400.18 MHz, 25 °C, TMS) δ 3.8 (CH_3), 8.7 (NH_2, H_2O). $^{13}C\{^1H\}$ NMR (DMSO-d_6, 100.63 MHz, 25 °C, TMS) δ 31.7 (CH_3), 148.5 (C-NH_2), 173.1 ([$N_4C-N{=}N-CN_4$]); ^{15}N NMR (solid state, 25 °C) δ −317.1 (−NH_2), −180.0 (N−CH_3), −71.2 (CNδ, −28.8 (−N = N−), +0.4 (CNα, +89.5 (−$N_{azo}{=}N_{azo}$−). Raman ($\tilde{\nu}$, cm^{-1}; rel. int.): 2961(3) 1487(58) 1420(14) 1382(100) 1356(3) 1191(1) 1084(10) 1058(47) 921(11) 790(6) 588(2) 328(1). IR ($\Delta\nu$, cm^{-1}; KBr, rel. int.): 3350(s) 2941(s) 2885(s) 2696(m) 2086(w) 1838(w) 1713(vs) 1663(m) 1528(m) 1454(m) 1429(m) 1416(m) 1398(s) 1253(w) 1198(m) 1178(w) 1156(m) 1081(w) 1061(w) 1048(w) 1026(w) 995(w) 922(w) 780(s) 730(m) 698(m) 586(w) 558(w) 517(w). *Decomposition Experiments.* MS (EI): *m/z* = 12 (0.2, C^{4+}), 13 (0.4, CH^{3+}), 14 (4.8, CH_2^{2+}, N^+), 15 (7.1, CH_3^+), 16 (8.4, $CH_4^{\cdot+}$, NH_2^+, O^{2+}), 17 (2.4, $NH_3^{\cdot+}$, OH^+), 18 (2.7, $H_2O^{\cdot+}$), 26 (2.8, CN^+), 27 (17.5, $HCN^{\cdot+}$), 28 (100.0, $N_2^{\cdot+}$), 38 (1.4, CCN^{3+}), 39 (1.9, $CHCN^{2+}$), 40 (4.5, CH_2CN^+), 41 (7.2, $CH_3CN^{\cdot+}$). IR (Gas): $\Delta\nu$ (cm^{-1}) = 3452 (vw, NH_3), 3332 (m, HCN), 3282 (m, HCN), 3083 (m, CH_4), 3011 (s, CH_4), 2951 (m, CH_4), 2166 (vw, HCN), 2102 (vw, HCN), 1621 (w, NH_3), 1430 (vw, HCN), 1381 (vw, HCN), 1302 (s, CH_4), 965 (vs, NH_3), 926 (vs, NH_3), 732 (m, HCN), 713 (vs, HCN), 682 (m, HCN), 629 (vw, NH_3).

Synthesis of 1,4-Dimethyl-5-aminotetrazolium Azotetrazolate (2). Method 1: Four equal portions of sodium azotetrazolate pentahydrate (total 1.003 g, 3.3 mmol) were suspended in 4 × 5 mL water in four separate plastic test-tubes. Silver nitrate (total 1.245 g, 7.3 mmol) was then added in approximately equal amounts to each tube. Immediate precipitation of highly sensitive silver azotetrazolate was observed and the four reaction mixtures were stirred for 15 min longer to ensure completion of the reaction. The mother liquors were centrifuged, and the remaining orange solid was washed twice with 5 mL of water with subsequent centrifuging. The water was eliminated by washing twice with 5 mL of dry methanol. The silver salt, wet with methanol, was suspended in 5 mL of fresh, dry methanol, and 1,4-dimethyl-5-aminotetrazolium iodide (1.590 g, 6.6 mmol) was added in equal portions to the reaction tubes. After a 30 min reaction time, yellow silver iodide was separated by filtration and the four methanol fractions were combined and rotavaporated to dryness, yielding yellow amorphous material, which was scratched out of the flask and recrystallized from little hot dry methanol (0.801 g, 62%). Crystals of **2** suitable for X-ray analysis were obtained when the same reaction was carried out in water and the solvent was left to slowly evaporate. Method 2: Alternatively, the water in **1** (1.151 g, 2.7 mmol) could be eliminated quantitatively when this was heated under a high vacuum at 80 °C for 7 days, yielding 1.048 g of pure product. $C_8H_{16}N_{20}$ (calcd/found): C 24.48/24.42, H 4.11/4.04, N 71.41/71.30. DSC (5 °C min^{-1}, °C): 193 (mp + dec.). *m/z* (FAB^+, xenon, 6 keV, m-NBA matrix): 114.2 $[DMAT]^+$; *m/z* (FAB^-, xenon, 6 keV, m-NBA matrix): 165.2 $[C_2N_{10}H]^-$. ^{1}H NMR (DMSO-d_6, 400.18 MHz, 25 °C, TMS) δ: 3.6 (CH_3), 8.5 (NH_2). $^{13}C\{^1H\}$ NMR (DMSO-d_6, 100.63 MHz, 25 °C, TMS) δ: 32.4 (CH_3), 148.8 (C−NH_2), 173.3 ([$N_4C-N{=}N-CN_4$]). Raman ($\tilde{\nu}$, cm^{-1}; rel. int.): 2951(2) 1490(25) 1468(22) 1410(14) 1378(100) 1353(4) 1197(2) 1082(8) 1066(14) 1057(30) 1031(7) 919(8) 791(5) 325(2) 271(1); IR ($\tilde{\nu}$, cm^{-1}; KBr, rel. int.): 3341(s) 3049(s) 2937(s) 2887(s) 2696(m) 1714(vs) 1663(m) 1528(m) 1453(m) 1430(m) 1416(m) 1398(s) 1348(w) 1253(w) 1198(m) 1178(w) 1156(m) 1080(w)

(23) http://www.linseis.net/html_en/thermal/dsc/dsc_pt10.php.
(24) (a) http://www.jeol.com/tabid/96/Default.aspx. (b) http://www.jeolusa.com/DesktopModules/Br ing2mind/DMX/Download.aspx?EntryId=331&PortalId=2&DownloadMethod=attachment. (c) http://www.jeoleuro.com/instr/mass/mass.htm.
(25) http://www.perkinelmer.com.
(26) http://www.parrinst.com.

1061(w) 1048(m) 1026(w) 995(m) 921(w) 789(s) 780(s) 730(s) 696(s) 586(w) 558(w) 517(w). *Decomposition Experiments.* MS (EI): m/z = 12 (0.2, C^{4+}), 13 (0.3, CH^{3+}), 14 (4.2, CH_2^{2+}, N^+), 15 (4.0, CH_3^+), 16 (5.1, $CH_4^{\cdot+}$, NH_2^+), 17 (5.1, $NH_3^{\cdot+}$), 26 (0.6, CN^+), 27 (1.1, $HCN^{\cdot+}$), 28 (100.0, $N_2^{\cdot+}$), 38 (0.7, CCN^{3+}), 39 (1.1, $CHCN^{2+}$), 40 (2.8, CH_2CN^+), 41 (5.0, $CH_3CN^{\cdot+}$). IR (Gas): $\Delta\nu$ (cm^{-1}) 3452 (vw, NH_3), 3334 (w, HCN), 3284 (vw, HCN), 3084 (m, CH_4), 3012 (s, CH_4), 2951 (m, CH_4), 2166 (vw, HCN), 2102 (vw, HCN), 1620 (w, NH_3), 1431 (vw, HCN), 1381 (vw, HCN), 1302 (s, CH_4), 966 (vs, NH_3), 926 (vs, NH_3), 732 (vw, HCN), 713 (w, HCN), 682 (vw, HCN), 668 (w, NH_3), 629 (w, NH_3).

Synthesis of 1,5-Diamino-4-methyl-tetrazolium Azotetrazolate Dihydrate (3). Sodium azotetrazolate pentahydrate (0.148 g, 0.5 mmol) was dissolved in 2 mL of hot water, and 1,5-diamino-4-methyltetrazolium iodide (0.244 g, 1.1 mmol) in 1 mL of hot water was added to the bright yellow solution. The reaction mixture was brought to boiling for 10 min and subsequently stored in a refrigerator for 1 h. Once again, the mixture was boiled for 15 min and left to slowly crystallize to room temperature in an oil bath and in the fridge for 2 h, yielding orange crystals suitable for X-ray structure analysis (0.153 g, 72%). $C_6H_{18}N_{22}O_2$ (calcd/found): C 16.74/16.88, H 4.22/4.21, N 71.61/71.32. DSC (5 °C min^{-1}, °C): 92 (-H_2O), 183 (mp + dec.); m/z (FAB^+, xenon, 6 keV, m-NBA matrix): 115.3 $[MeDAT]^+$; m/z (FAB^-, xenon, 6 keV, m-NBA matrix): 165.2 $[C_2N_{10}H]^-$; ^{1}H NMR (DMSO-d_6, 400.18 MHz, 25 °C, TMS): δ 3.9 (CH_3), 7.2 (NH_2, H_2O). $^{13}C\{^1H\}$ NMR (DMSO-d_6, 100.63 MHz, 25 °C, TMS) δ: 34.5 (CH_3), 147.7 (C-NH_2),173.2 ([$N_4C-N{=}N-CN_4$]); ^{15}N NMR (solid state, 25 °C): δ −317.0 (C−NH_2), −308.9 (N−**N**H_2), −180.8 (N−CH_3), −170.7 (**N**−NH_2), −82.1 (CNδ, −58.7 (N13), −47.2 (N14), −0.3 (CNδ, +90.1 (−N_{azo}=N_{azo}−). Raman ($\tilde{\nu}$, cm^{-1}; rel. int.): 2972(6) 1479(46) 1422(19) 1382(100) 1089(17) 1057(44) 921(12) 790(7) 278(5); IR ($\tilde{\nu}$, cm^{-1}; KBr, rel. int.): 3345(s) 3193(s) 3063(s) 2958(s) 2087(w) 1721(vs) 1627(w) 1499(w) 1450(w) 1416(m) 1400(s) 1384(m) 1245(w) 1213(w) 1192(w) 1157(w) 1114(w) 1083(w) 1048(w) 1040(w) 1001(w) 923(w) 875(w) 787(m) 756(m) 732(m) 681(m) 597(w) 559(w) 531(w). *Decomposition Experiments.* MS (EI): m/z = 12 (0.8, C^{4+}), 13 (0.3, CH^{3+}), 14 (3.8, CH_2^{2+}, N^+), 15 (1.1, CH_3^+), 16 (3.9, $CH_4^{\cdot+}$, NH_2^+, O^{2+}), 17 (4.7, $NH_3^{\cdot+}$, OH^+), 18 (1.5, $H_2O^{\cdot+}$), 26 (4.5, CN^+), 27 (26.1, $HCN^{\cdot+}$), 28 (100.0, $N_2^{\cdot+}$), 44 (2.3, $N(CH_3)_2^+$). IR (Gas): $\Delta\nu$ (cm^{-1}) 3450 (vw, NH_3), 3330 (w, HCN), 3282 (w, HCN), 3083 (w, CH_4), 3012 (w, CH_4), 2918 (vw, CH_4), 2850 (m, $HN(CH_3)_2$), 2810 (m, $HN(CH_3)_2$), 2166 (w, HCN), 2102 (w, HCN), 1621 (w, NH_3), 1430 (vw, HCN), 1380 (vw, HCN), 1302 (w, CH_4), 965 (s, NH_3), 926 (s, NH_3), 732 (m, HCN), 713 (vs, HCN), 682 (w, HCN), 667 (w, NH_3), 629 (w, NH_3).

Synthesis of 1,5-Diamino-4-methyl-tetrazolium Azotetrazolate (4). Method 1: Sodium azotetrazolate pentahydrate (0.522 g, 1.7 mmol) was reacted with silver nitrate (0.311 g, 1.8 mmol) in 5 mL of water, causing immediate precipitation of orange highly sensitive silver azotetrazolate. The reaction mixture was stirred for 5 min and centrifuged. The solvent was decanted off and the silver salt was freed of excess silver nitrate by washing with 5 mL of water and subsequently centrifuging. The water was eliminated by washing twice with 5 mL of dry methanol. The metathesis reaction was carried out in 5 mL dry methanol by addition of neat 1,5-diamino-4-methyltetrazolium iodide (0.300 g, 1.2 mmol) and stirring for 15 min. Yellow silver iodide was filtered and the solvent was removed under a high vacuum, leaving a yellow crude product that could be recrystallized by ether diffusion into a small amount of methanol. Yellow crystals suitable for X-ray analysis and powdery material formed overnight (0.312 g, 64%). Method 2: Alternatively the dihydrated species **3** (1.081 g, 2.5 mmol) could be freed from water by heating at 80 °C under a high vacuum for 5 days, yielding 0.989 g of the product (quantitative yield). $C_6H_{14}N_{22}$ (calcd/found): C 18.26/18.26, H 3.58/3.59, N 78.15/77.34. DSC (5 °C min^{-1}, °C): 170 (mp + dec); m/z (FAB^+, xenon, 6 keV, m-NBA matrix): 115.3 $[MeDAT]^+$; m/z (FAB^-, xenon, 6 keV, m-NBA matrix): 165.2 $[C_2N_{10}H]^-$. ^{1}H NMR (DMSO-d_6, 400.18 MHz, 25 °C, TMS): δ 3.9 (CH_3), 6.9 (NH_2); $^{13}C\{^1H\}$ NMR (DMSO-d_6, 100.63 MHz, 25 °C, TMS): δ 34.9 (CH_3), 147.5 (C−NH_2), 173.3 ([$N_4C-N{=}N-CN_4$]); Raman ($\tilde{\nu}$, cm^{-1}; rel. int.): 2969(1) 1484(52) 1414(9) 1380(100) 1353(3) 1196(1) 1158(1) 1074(16) 1049(26) 1030(5) 920(7) 790(4) 732(1) 605(1) 328(2); IR ($\tilde{\nu}$, cm^{-1}; KBr, rel. int.): 3737(s) 3378(s) 3259(s) 2968(s) 2786(s) 2630(m) 2419(m) 2225(w) 1709(vs) 1643(m) 1603(m) 1497(w) 1456(m) 1443(m) 1427(m) 1388(sm) 1245(w) 1193(m) 1157(m) 1119(m) 1067(w) 1039(m) 1031(m) 1008(m) 934(m) 782(m) 736(m) 725(m) 694(m) 663(m) 602(w) 555(m) 527(m) 516(m). *Decomposition Experiments.* MS (EI): m/z = 12 (0.4, C^{4+}), 13 (0.1, CH^{3+}), 14 (3.4, CH_2^{2+}, N^+), 15 (0.1, CH_3^+), 16 (1.1, $CH_4^{\cdot+}$, NH_2^+), 17 (1.4, $NH_3^{\cdot+}$), 26 (1.3, CN^+), 27 (8.3, $HCN^{\cdot+}$), 28 (100.0, $N_2^{\cdot+}$), 44 (2.7, $N(CH_3)_2^+$). IR (Gas): $\Delta\nu$ (cm^{-1}) 3450 (vw, NH_3), 3330 (w, HCN), 3282 (w, HCN), 3083 (vw, CH_4), 3012 (vw, CH_4), 2951 (vw, CH_4), 2917 (w, $HN(CH_3)_2$), 2849 (w, $HN(CH_3)_2$), 2166 (w, HCN), 2103 (w, HCN), 1622 (w, NH_3), 1430 (vw, HCN), 1380 (vw, HCN), 1302 (vw, CH_4), 965 (s, NH_3), 926 (s, NH_3), 732 (m, HCN), 713 (vs, HCN), 682 (m, HCN), 668 (w, NH_3), 629 (w, NH_3).

Scheme 1. Synthesis of the Nitrogen-Rich Azotetrazolate Salts 1–4

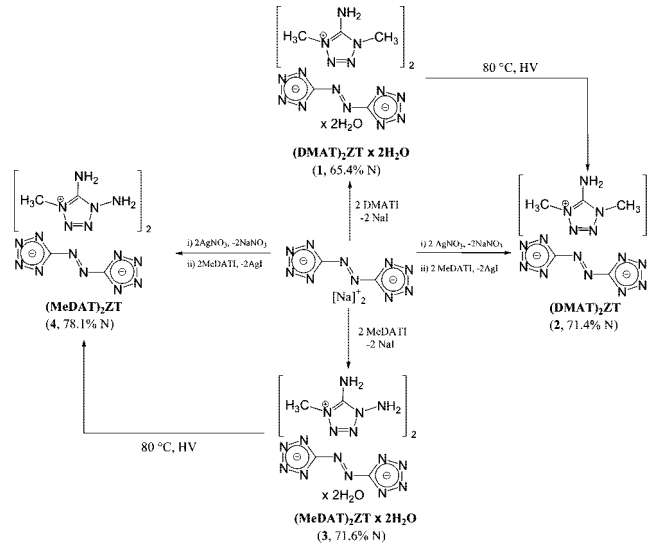

Results and Discussion

Synthesis. As is usual for azotetrazolate salts when the synthesis is carried out in aqueous solution, the compounds incorporate crystal water in the structure.[1c,12] The 1,4-dimethyl-5-aminotetrazolium and 1,5-diamino-4-methyltetrazolium azotetrazolate species **1** and **3** could be obtained by recrystallization from water of equimolar amounts of sodium 5,5′-azotetrazolate and the appropriate tetrazolium iodide as the dihydrated species (Scheme 1). On cooling, **1** precipitated as a yellow powder, whereas **3** crystallized as a slightly orange solid, both in yields >70%. **2** and **4** were synthesized in moderate yield by a metathesis reaction between highly sensitive silver 5,5′-azotetrazolate (Ag_2ZT), generated from Na_2ZT and silver nitrate, and the corresponding tetrazolium iodide in dry methanol. Alternatively, the

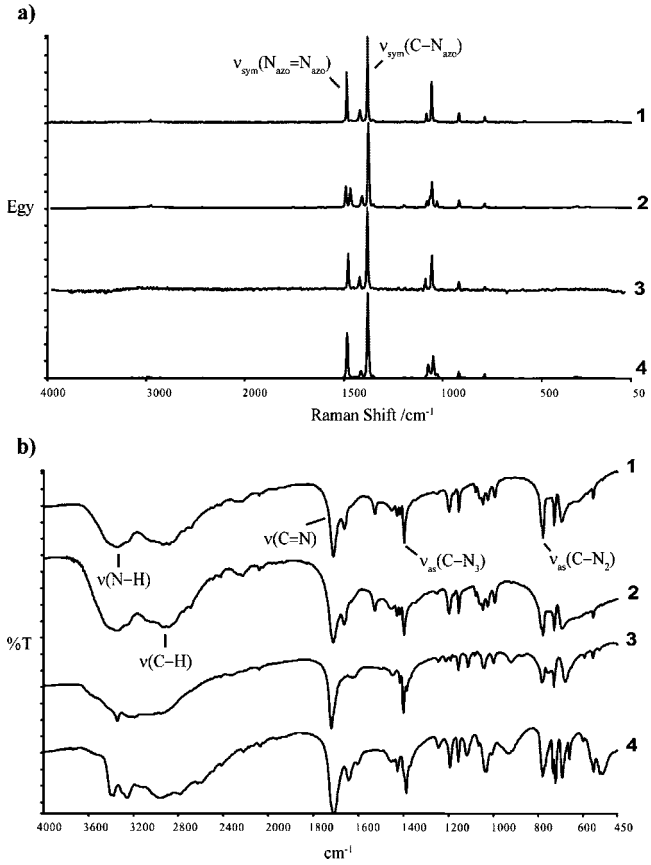

Figure 1. (a) Raman and (b) IR spectra of nitrogen-rich azotetrazolate salts **1–4**.

two molecules of crystal water in **1** and **3** could be removed by heating to temperatures around 80 °C for several days under a high vacuum, yielding the anhydrous species **2** and **4** in quantitative isolated yield and providing a much more efficient and safer method for their syntheses on a larger scale.

Vibrational and NMR Spectroscopy. Intense signals in the Raman spectra of salts **1**-**4** corresponding to the symmetric C-N_{azo} stretching (~1380 cm^{-1}) and the stretching mode of the azo group (~1480 cm^{-1}) obscure the bands corresponding to the cation (Figure 1a). The Raman spectra of all four compounds have identical shapes, and only slight differences in vibrational energies are observed (see Experimental Section). The formation of the tetrazolium azotetrazolate compounds is easily confirmed by comparing the Raman spectra of the reaction products with those of the starting materials. The two bands centered at ~1060 and ~1090 cm^{-1} for **1**−**4** are shifted in respect to the sodium salt (1068 and 1099 cm^{-1}) and have exchanged their relative intensities. The IR spectra of all compounds show the characteristic bands of the 5,5′-azotetrazolate anion for the asymmetric C−N_3 (~1400 cm^{-1}) and the asymmetric C−N_2 (~730 cm^{-1}) stretching modes. However, the most intense peak in the IR spectra can be assigned to the stretching mode in the cation between the tetrazole carbon and the exocyclic imino nitrogen atoms (~1715 cm^{-1} [ν(C3═N11)]). The IR and Raman spectra also contain other sets of bands of lower intensity that can be assigned to the cations: 3400–3100 cm^{-1} [ν(N−H)], 3000–2850 cm^{-1} [ν(C−H)], 1680–1550 [δ(N11H_2), δ(N16H_2)], 1550–1350 cm^{-1} [ν(tetrazole ring), δ_{as}(CH_3)], ~1380 cm^{-1} [δ(CH_3)], 1350–700 cm^{-1} [ν(N12−C3−N15), ν(N−N), γ(CN), δ(tetrazole ring)], <700 cm^{-1} [δ out-of-plane bend (N−H), ω(N11H_2)].[22,27,28]

The IR spectra (Figure 1b) also provide insight into the cation structure and hydrogen bonding.[29] The free base of **1** and **2** (1,4-dimethyl-5-imino-*1H*-tetrazole, **5**) shows one only sharp band at 3314 cm^{-1}[30a] corresponding to the N11-H stretching, which upon formation of the azotetrazolate salts **1** and **2**splits in two sets of broad bands centered at ~3345 and ~3210 cm^{-1}, indicative of the formation of NH_2 group extensive hydrogen bonding as confirmed by the crystal structures. The most intense peak in the IR spectrum of **5** corresponds to the C3═N11H stretching vibration (1649 cm^{-1}), which is shifted to significantly higher energies in **1** (1713 cm^{-1}) and **2** (1714 cm^{-1}), indicating variations in the C3═N11 distances between DMAT$^+$ and **5** and proving again the existence of strong hydrogen-bonding. In analogy to **1** and **2**, the IR spectrum of the free base of **3** and **4** (1-amino-4-methyl-5-imino-*1H*-tetrazole, **6**) shows a sharp band at 3281 cm^{-1},[30b] which is split into two centered at ~3360 and ~3225 cm^{-1}. The C3═N11H stretching of the free base **6** (1670 cm^{-1}) is once again shifter to higher energies in **3** (1721 cm^{-1}) and **4** (1709 cm^{-1}).

In the ^{1}H NMR, the signals corresponding to the methyl groups are found just below 4.0 ppm (Table 1). For compounds **3** and **4**, the substitution of one of the methyl groups in **1** and **2** by an amino group has a slight deshielding effect on the methyl groups and as a consequence they appear at slightly lower field. There seems to be fast exchange in DMSO-d_6 since the crystal water is seen as one only broad signal together with the amino groups. The 1-amino and 5-amino groups in the case of the MeDAT$^+$ derivatives also suffer from fast exchange and are shifted to higher field in comparison to the 5-amino group in the DMAT$^+$ salts (~7.0 vs ~8.6 ppm). In the ^{13}C NMR, the shifts are very similar to the starting materials. Resonances for the two azotetrazolate carbon atoms are found around 173 ppm and the tetrazole sp^2-hybridized carbon atoms are found around 148 ppm in all four compounds, but at slightly lower field in the case of the dimethylated species **1** and **2**. However, the methyl groups appear at lower field in the case of the diaminated salts **3** and **4** (~34.5 ppm) in comparison to the dimethylated species (~32.0 ppm).

The quadrupolar broadening found in the ^{14}N NMR does not allow the differentiation of any signal from the baseline and all compounds were not soluble enough in any solvent to record a ^{15}N NMR (natural abundance). Figure 2 shows the ^{15}N NMR spectrum of compound **1** in the solid state. The resonances for the cation are sharp and split because of differences in the interactions in the crystal structure (see Crystal Structures section). They are centered at −317.1 (−NH_2), −180.0 (N-CH_3), and −28.8 (−*N*═N−) ppm in agreement with the ^{15}N NMR in DMSO-d_6 solution of other compounds containing the same cation,[27] whereas the lack

(27) Karaghiosoff, K.; Klapötke, T. M.; Mayer, P.; Miró-Sabaté, C.; Penger, A.; Welch, J. M. *Inorg. Chem.* **2007**, in press.
(28) Colthup, N. B.; Daly, L. H.; Wiberley, S. E. *Introduction to Infrared and Raman Spectroscopy*l Academic Press: Boston, 1990.
(29) Jeffrey, G. A. *An Introduction to Hydrogen Bonding*; Oxford University Press: New York, 1997.

Table 1. Characterization of the Nitrogen-Rich Azotetrazolate Salts 1–4

param	1	2	3	4
^{1}H NMR (ppm)	3.8 (CH_3)	3.6 (CH_3)	3.9 (CH_3)	3.9 (CH_3)
	8.7 (NH_2, H_2O)	8.5 (NH_2)	7.2 (NH_2, H_2O)	6.9 (NH_2)
^{13}C NMR (ppm)	31.7 (CH_3)	32.4 (CH_3)	34.5 (CH_3)	34.9 (CH_3)
	148.5 (C-NH_2)	148.8 (C-NH_2)	147.7 (C-NH_2)	147.5 (C-NH_2)
	173.1 ($[C_2N_{10}]^{2-}$)	173.3 ($[C_2N_{10}]^{2-}$)	173.2 ($[C_2N_{10}]^{2-}$)	173.3 ($[C_2N_{10}]^{2-}$)
IR (cm^{-1})	1399, 731	1398, 730	1401, 731	1400, 731
Raman (cm^{-1})	1487, 1382	1490, 1379	1479, 1382	1479, 1382
mass spectrometry	114 (cation, FAB^+)	114 (cation, FAB^+)	115 (cation, FAB^+)	115 (cation, FAB^+)
	165 ($[C_2N_{10}H]^-$, FAB)	165 ($[C_2N_{10}H]^-$, FAB^-)	165 ($[C_2N_{10}H]^-$, FAB^-)	165 ($[C_2N_{10}H]^-$, FAB^-)
DSC (°C, 5 °C min^{-1})	84 ($-H_2O$)	193 (mp + dec.)	92 (-H_2O)	170 (mp + dec)
	197 (mp + dec.)		183 (mp + dec.)	
elemental analysis (%, calcd/found)	N (65.40/65.68)	N (71.41/71.30)	N (71.61/71.32)	N (78.15/77.34)
	C (22.42/22.49)	C (24.48/24.42)	C (16.74/16.88)	C (18.26/18.26)
	H (4.71/4.60)	H (4.11/4.04)	H (4.22/4.21)	H (3.58/3.59)

Table 2. Crystal Data and Structure Refinement for Nitrogen-Rich Azotetrazolate Salts 1–4

param	1	2	3	4
formula	$C_8H_{20}N_{20}O_2$	$C_8H_{16}N_{20}$	$C_6H_{18}N_{22}O_2$	$C_6H_{14}N_{22}$
fw	428.44	392.35	430.35	394.39
cryst size (mm^3)	0.05 × 0.02 × 0.02	0.05 × 0.1 × 0.08	0.1 × 0.05 × 0.04	0.01 × 0.02 × 0.05
T (K)	200(2)	200(2)	200(2)	200(2)
cryst syst	monoclinic	triclinic	triclinic	triclinic
space group	$P2_1/c$	$P\bar{1}$	$P\bar{1}$	$P\bar{1}$
a (Å)	14.441(3)	5.830(4)	7.505(2)	5.840(5)
b (Å)	9.277(2)	10.994(8)	8.184(2)	11.008(5)
c (Å)	16.014(3)	14.71(1)	9.040(2)	14.727(5)
α (deg)	90	99.93(1)	108.58(3)	99.93(1)
β (deg)	113.01(3)	93.64(1)	112.70(3)	93.63(1)
γ (deg)	90	98.72(1)	98.25(3)	98.69(1)
V (Å^3)	1974.7(7)	913.8(2)	462.3(1)	918.0(9)
Z	4	2	1	2
ρ (g cm^{-3})	1.441	1.431	1.546	1.427
λ (Mo Kα, Å)	0.71073	0.71073	0.71073	0.71073
μ (mm^{-1})	0.114	0.108	0.125	0.111
no. of reflns collected	7180	10071	6358	12572
no. of ind. reflns	2045	2928	2232	2961
R_{int}	0.0530	0.0664	0.0616	0.0423
no. of obsd reflns	3871	3939	2704	5347
F(000)	896	400	224	408
GOF	1.066	1.024	1.109	1.018
R_1/wR_2 [$I > 2\sigma(I)$]	0.0606/0.1528	0.0556/0.1192	0.0471/0.1244	0.0618/0.1573
R_1/wR_2 (all data)	0.1347/0.1871	0.1008/0.1446	0.0616/0.1364	0.1208/0.1939
no. of params	287	317	172	271
CCDC no.	662750	662751	662752	662753

of protons on the azotetrazolate anion make the corresponding signals rather broad and low in intensity. Alike the cation, the anion in **1** also shows three resonances corresponding to the azo bridge nitrogen (+89.5 ppm), the ring α-nitrogen (+0.4 ppm) and the ring β-nitrogen (−71.2 ppm) atoms[13]. The solid-state ^{15}N NMR spectrum of **2** shows even broader signals corresponding to the azotetrazolate anion resonances and just the cation shifts can be easily identified. They occur

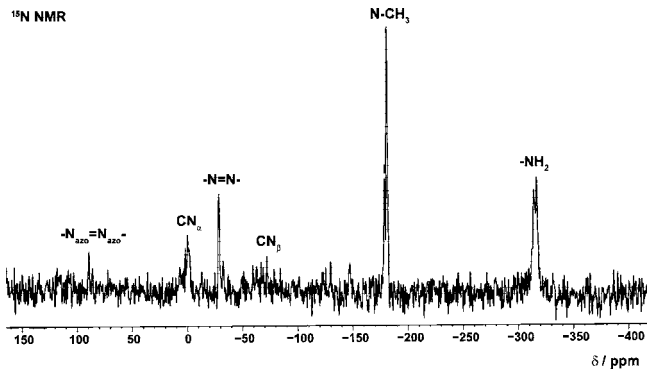

Figure 2. Solid-state ^{15}N NMR spectrum of azotetrazolate salt **1**.

at −317.0 (C−NH_2), −308.9 (N−**N**H_2), −180.8 (N−CH_3), −170.7 (**N**−NH_2), −58.7 (N13), and −47.2 (N14) ppm, in accordance with other $MeDAT^+$ salts.[22]

Crystal Structures. Crystals of the nitrogen-rich azotetrazolate salts **1**–**4** were obtained as described in the experimental section. The X-ray crystallographic data for **1** (CCDC 662750) and **2** (CCDC 662751) were collected on an Enraf-Nonius Kappa CCD diffractometer. Data sets for **3** (CCDC 662752), and **4** (CCDC 662753) were collected on an Oxford Diffraction Xcalibur 3 diffractometer equipped with a CCD detector. All data were collected using graphite-monochromated Mo Kα radiation (λ = 0.71073 Å). No absorption corrections were applied to data sets collected for any of the compounds. All structures were solved by direct methods (SHELXS-97 and SIR97)[31] and refined by means of full-matrix least-squares procedures using SHELXL-97. Crystallographic data are summarized in Table 2. Selected bond lengths and angles are reported in Tables 3−6 and hydrogen-bonding geometries in Table 7. All non-hydrogen atoms were refined anisotropically. For all compounds, all hydrogen atoms were located from difference Fourier electron-density

Table 3. BondDistances (Å) in the Azotetrazolate Anions of Nitrogen-Rich Salts 1–4

bond	**1**[a]	**2**[b]	**3**[c]	**4**[d]
N1−N2	1.336(4)	1.326(1)	1.345(2)	1.333(3)
N1−C1	1.331(4)	1.326(1)	1.336(2)	1.335(3)
N2−N3	1.319(4)	1.325(1)	1.321(2)	1.322(3)
N3−N4	1.347(4)	1.335(1)	1.335(2)	1.336(3)
N4−C1	1.321(4)	1.332(1)	1.330(2)	1.339(3)
N5−C1	1.402(4)	1.417(1)	1.411(2)	1.415(3)
N5−A	1.265(3)	1.245(1)	1.258(2)	1.250(3)
N6−C2	1.402(4)	1.407(1)		1.399(3)
C2−N7	1.333(4)	1.325(1)		1.332(3)
N7−N8	1.334(4)	1.334(1)		1.336(3)
N8−N9	1.318(4)	1.318(1)		1.324(3)
N9−N10	1.345(3)	1.341(1)		1.337(3)
N10−C2	1.323(4)	1.333(1)		1.344(3)
N6−B		1.265(1)		1.262(3)

[a] **1**: A = N6. [b] **2**: A = N5^{i}, B = N6^{ii} (symmetry codes: (i) 1 − *x*, 1 − *y*, 1 − *z*; (ii) –1 − *x*, −*y*, −*z*). [c] **3**: A = N5^{i} (symmetry code: (i) 2 − *x*, −*y*, 1 − *z*). [d] **4**: A = N5^{i}, B = N6^{ii} (symmetry codes: (i) 1 − *x*, –2 − *y*, 2 − *z*; (ii) 1 − *x*, –1 − *y*, 1 − *z*).

Table 4. Bond Angles (deg) in the Azotetrazolate Anions of Nitrogen-Rich Salts 1–4

angle	**1**[a]	**2**[b]	**3**[c]	**4**[d]
C1−N5−A	112.5(2)	112.5(2)	113.0(1)	112.4(2)
C1−N1−N2	104.9(3)	104.4(1)	103.6(1)	103.6(2)
N3−N2−N1	108.6(2)	109.3(1)	110.2(1)	109.9(2)
C1−N4−N3	103.9(2)	103.4(1)	105.1(1)	104.0(2)
N2−N3−N4	109.9(3)	109.9(1)	108.8(1)	109.7(2)
N4−C1−N1	112.6(3)	113.0(2)	112.3(1)	112.8(2)
N4−C1−N5	128.9(3)	129.4(2)	128.1(1)	129.8(2)
N1−C1−N5	118.5(3)	117.6(2)	118.5(1)	117.4(2)
C2−N6−B	112.9(3)	112.5(2)		113.3(2)
N8−N9−N10	109.8(3)	109.2(1)		109.7(2)
C2−N7−N8	104.5(3)	104.1(1)		104.4(2)
C2−N10−N9	103.8(2)	104.0(1)		104.0(2)
N9−N8−N7	109.2(2)	109.9(1)		109.6(2)
N10−C2−N7	112.7(3)	112.8(2)		112.2(2)
N10−C2−N6	128.8(3)	127.3(2)		120.5(2)
N7−C2−N6	118.4(3)	119.9(2)		127.3(2)

[a] **1**: A = N6, B = N5. [b] **2**: A = N5^{i}, B = N6^{ii} (symmetry codes: (i) 1 − *x*, 1 − *y*, 1 − *z*; (ii) –1 − *x*, −*y*, −*z*). [c] **3**: A = N5^{i} (symmetry code: (i) 2 − *x*, −*y*, 1 − *z*). [d] **4**: A = N5^{i}, B = N6^{ii} (symmetry codes: (i) 1 − *x*, –2 − *y*, 2 − *z*; (ii) 1 − *x*, –1 − *y*, 1 − *z*).

Table 5. BondDistances (Å) in the Cations of Nitrogen-Rich Azotetrazolate Salts 1–4

bond	**1**[a]	2[a]	3[b]	4[c]
C3−N11	1.310(5)	1.309(1)	1.313(1)	1.312(3)
C3−N12	1.339(5)	1.336(1)	1.338(1)	1.343(3)
C3−N15	1.339(5)	1.344(1)	1.347(1)	1.343(3)
N12−N13	1.371(5)	1.361(1)	1.374(1)	1.366(3)
N13−N14	1.274(5)	1.273(1)	1.268(1)	1.270(3)
N14−N15	1.366(5)	1.360(1)	1.375(1)	1.361(3)
N12−R_1	1.449(5)	1.447(1)	1.455(1)	1.454(3)
N15−R_2	1.446(5)	1.451(1)	1.383(1)	1.449(3)
C5−N17	1.310(5)	1.312(1)		1.307(3)
C5-N18	1.334(5)	1.337(1)		1.340(2)
C5−N21	1.338(5)	1.339(1)		1.345(3)
N18−N19	1.374(5)	1.361(1)		1.370(3)
N19−N20	1.273(5)	1.271(1)		1.279(3)
N20−N21	1.364(5)	1.368(1)		1.363(3)
N18−R_3	1.456(5)	1.450(1)		1.455(3)
N21−R_4	1.453(5)	1.447(1)		1.445(3)

[a] **1** and **2**: R_1 = C4, R_2 = C5, R_3 = C7, R_4 = C8. [b] **3**: R_1 = C4, R_2= N16. [c] **4**: R_1 = C4/N16, R_2 = N16/C4, R_3 = C7/N22, R_4 = N22/C7.

Table 6. Bond angles (deg) in the Cations of Nitrogen-Rich Azotetrazolate Salts 1–4

angle	**1**[a]	2[a]	3[b]	4[c]
N12−C3−N11	127.1(3)	127.2(2)	127.2(1)	128.1(2)
N15−C3−N11	127.8(3)	128.2(2)	128.3(1)	127.1(2)
C3−N12−R_1	128.6(3)	128.6(2)	128.9(1)	128.4(2)
N13−N12−R_1	122.3(2)	122.0(2)	121.4(1)	122.0(2)
C3−N12−N13	109.1(3)	109.3(2)	109.6(1)	109.5(2)
N12−N13−N14	108.3(3)	108.3(2)	108.5(1)	108.0(2)
N13−N14−N15	108.0(3)	107.9(2)	107.7(1)	108.2(2)
N14−N15−C3	109.5(2)	109.9(2)	109.(1)	109.5(2)
C3−N15−R_2	129.0(3)	128.7(2)	128.5(1)	128.4(2)
N4−N15−R_2	121.4(3)	121.4(2)	121.4(1)	122.1(2)
N12−C3−N15	105.1(3)	104.5(2)	104.4(1)	104.8(2)
N18−C6−N17	128.5(3)	127.2(2)		127.4(2)
N21−C6−N17	127.0(3)	127.7(2)		127.9(2)
C6−N18−R_3	129.4(3)	128.2(2)		128.8(2)
N19−N18−R_3	120.6(3)	122.3(2)		122.3(2)
C6−N18−N19	110.0(3)	109.5(2)		109.2(2)
N18−N19−N20	108.1(2)	108.2(2)		108.4(2)
N19−N20−N21	107.6(3)	108.2(2)		108.3(2)
N20−N21−C6	109.8(3)	109.0(2)		109.5(2)
C6−N21−R_4	129.6(2)	128.5(2)		128.5(2)
N20−N21−R_4	120.5(3)	122.4(2)		121.7(2)
N18−C6−N21	104.5(3)	105.1(2)		104.7(2)

[a] **1** and **2**: R_1 = C4, R_2 = C5, R_3 = C7, R_4 = C8. [b] **3**: R_1 = C4, R_2= N16. [c] **4**: R_1 = C4/N16, R_2 = N16/C4, R_3 = C7/N22, R_4 = N22/C7.

Table 7. Hydrogen-Bonding Geometry in Nitrogen-Rich Azotetrazolate Salts 1–4[a]

D−H···A	D−H (Å)	H···A (Å)	D···A (Å)	D−H···A (deg)
		1		
O1−H1A···N4	0.85(4)	2.01(4)	2.850(5)	177(4)
O2−H2B···N10	0.81(4)	2.13(4)	2.933(5)	170(3)
N17−H17B···N1^{i}	0.86(3)	2.03(3)	2.889(4)	174(2)
N17−H17A···O2^{i}	0.86(3)	1.85(3)	2.739(4)	166(2)
N11−H11A···O1^{ii}	0.86(3)	1.85(3)	2.704(4)	170(2)
N11−H11B···N7^{ii}	0.86(3)	2.02(3)	2.876(4)	170(2)
O2−H2A···N3^{iii}	0.95(6)	1.87(6)	2.793(4)	168(5)
O1−H1B···N9^{v}	0.99(5)	1.83(5)	2.818(4)	176(4)
		2		
N11−H11A···N3	0.87(1)	2.01(2)	2.860(2)	165(1)
N11−H11B···N7	0.93(1)	1.93(1)	2.849(2)	169(1)
N17−H17A···N2^{iii}	0.84(1)	2.08(1)	2.922(2)	171(1)
N17−H17B···N8^{iii}	0.92(1)	1.97(2)	2.885(2)	179(1)
		3		
N11−H11A···N16	0.88(3)	2.63(1)	2.912(1)	100(3)
N11–11B···O1^{viii}	0.91(1)	1.88(1)	2.784(1)	172(1)
N16−H16B···N1^{viii}	0.84(1)	2.43(1)	3.168(1)	146(1)
O1−H1B···N2^{viii}	0.88(1)	1.93(1)	2.832(1)	173(1)
N11−H11A···N4^{xiii}	0.88(1)	2.03(1)	2.892(2)	164(2)
O1−H1A···N1^{xiv}	0.80(1)	2.04(1)	2.806(1)	170(1)
N16−H16A···O1^{xv}	0.88(1)	2.19(1)	3.024(1)	159(1)
		4		
N11−H11A···N3^{vii}	0.80(2)	2.13(2)	2.929(3)	170(2)
N17−H17A···N2^{vii}	0.84(2)	2.04(2)	2.863(3)	165(3)
N11−H11B···N8^{viii}	0.95(3)	1.95(3)	2.884(3)	167(2)
N17−H17B···N7^{viii}	0.83(3)	2.03(2)	2.852(3)	168(3)

[a] Symmetry codes for **1**: (i) *x*, −0.5 − *y*, 0.5 + *z*; (ii) *x*, −0.5 − *y*, −0.5 + *z*; (iii) *x*, −1 + *y*, *z*; (v) *x*, 1 + *y*, *z*; **2**: (iii) 1 − *x*, 1 − *y*, 1 − *z*; **3**: (viii) 1 − *x*, 1 − *y*, −*z*; (xiii) −1 + *x*, *y*, −1 + *z*; (xiv) *x*, 1 + *y*, *z*; (xv) −1 + *x*, *y*, *z*; **4**: (vii) 1 + *x*, *y*, *z*; (viii) 1 − *x*, 1 − *y*, 1 − *z*.

maps and refined isotropically. Further information on the crystal-structure determinations (excluding structure factors) has been deposited at the Cambridge Crystallographic Data Centre and is available free of charge by request from CCDC, 12 Union Road, Cambridge CB2 1EZ, U.K. (fax (44) 1223–336–033, e-mail deposit@ccdc.cam.ac.uk).

1 crystallizes in the monoclinic system (space group $P2_1/c$), whereas the remainder of the compounds have triclinic cells and crystallize in the same space group ($P\bar{1}$). **1**, as would be expected from the greater number of molecules in the unit cell ($Z = 4$) has the largest cell volume, whereas **3** with

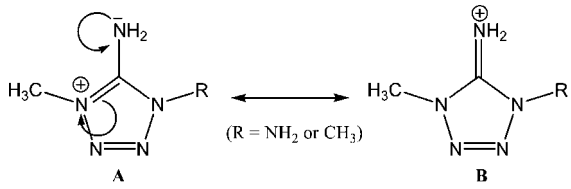

Figure 3. Aromatic delocalization in the tetrazolium cation of nitrogen-rich azotetrazolates salts **1**–**4**.

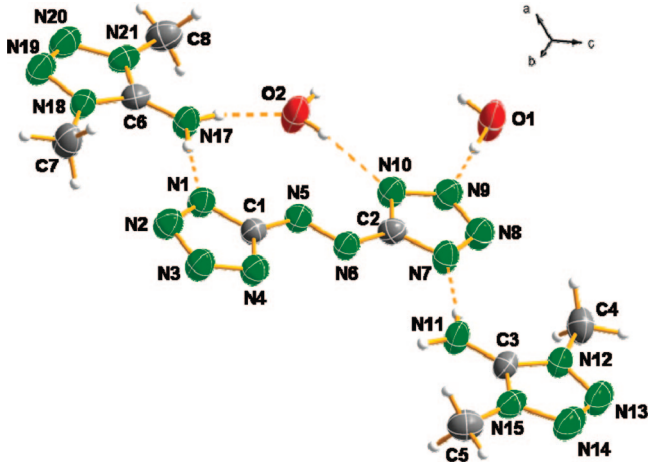

Figure 4. Asymmetric unit of azotetrazolate **1** with hydrogen bonding (dotted lines) and the labelling scheme (ellipsoids are represented at the 50% probability level).

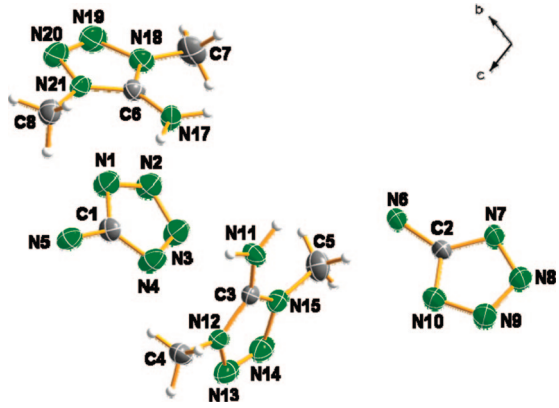

Figure 5. Asymmetric unit of azotetrazolate **2** with the labelling scheme (view along *a*, ellipsoids are represented at the 50% probability level).

$Z = 1$, has the smallest. **2** and **4** have very similar cell parameters (both almost identical cell lengths and identical angles) as well as very similar hydrogen-bonding networks (a graph-set analysis of the hydrogen-bonding patterns follows below).

The asymmetric units (ASU) of compounds **1**-**3** are shown as Diamond projections in Figures 4−6. A representation of the ASU for salt **4** was omitted because of the fact that the compound crystallizes with the methyl and amino groups disordered. Interatomic distances (Table 3) and angles (Table 4) for the 5,5′-azotetrazolate anions in compounds **1**–**4** are very similar. The N−N distances on the tetrazole rings, between 1.317(3) and 1.345(3) Å, are longer than normal *C*═N double bonds (1.22 Å) and shorter than normal C−N

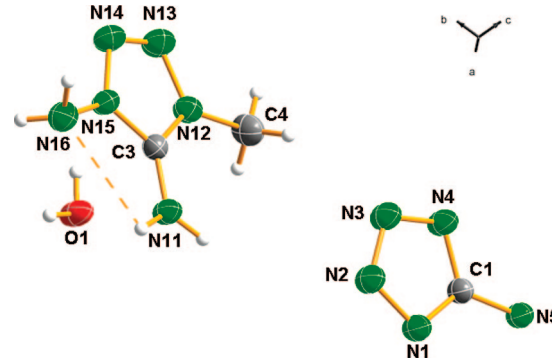

Figure 6. Asymmetric unit of azotetrazolate **3** showing the N11−N16 intramolecular hydrogen bond and the labelling scheme (ellipsoids are represented at the 50% probability level).

single bonds (1.47 Å),[32] implying a certain delocalization throughout the tetrazole ring. The azo-bridge N−N distances between 1.250(2) and 1.265(3) Å are slightly longer than a typical *N*═N double bond showing the aromatic character of the anion.[33] Both distances compare nicely with the values measured for the crystal structures of azotetrazolate salts with alkali and earth-alkali metals[1c] and other salts containing the same anion.[15,18] The geometry of the cations is summarized in Tables 5 and 6. Within the uncertainty of the experiment, all parameters agree with the previously reported distances for salts containing the $DMAT^{+}$[2,21] and $MeDAT^{+}$[22,34] cations. The C3−N11 (C6−N17) and N13−N14 (N19−N20) distances suggest a partial localization of the double bond character in these two bonds making the imino form B (Figure 3) a more suitable structure to describe the bonding situation in the solid-state structure of compounds **1**−**4**, as seen in other tetrazolium salts.[22,27,34]

The 5,5′-azotetrazolate anions in the dihydrated species **1** and **3** are connected to water molecules through hydrogen bonds forming layers with alternating cations and anions joined by the water molecules (Figures 7 and 8). Each water molecule participates in three different hydrogen bonds (two as the donor and one as the acceptor). The water molecules have H-O-H angles of 99° in **1** and 103° in **3**. In the case of **1** the asymmetric unit describes a complete formula moiety (two cations, one anion. and two water molecules; see Figure 4). Four different hydrogen bonds to four water molecules with distances between donor and acceptor atoms (N−H···O) ranging from 2.793(4) to 2.933(4) Å (Table 7) are observed. In addition, there are two hydrogen bond types between water molecules and amino groups with D–A distances of 2.704(4) and 2.740(4) Å. The remaining hydrogen atoms of the amino

(30) (a) Klapötke, T. M.; Miró-Sabaté, C.; Welch, J. M. **2007**, unpublished results. (b) Klapötke, T. M.; Miró-Sabaté, C.; Welch, J. M. *Z. Anorg. Allg. Chem.* **2007**, submitted.
(31) (a) Sheldrick, G. M. *Programs for Crystal Structure Analysis (Release 97–2)*; Institüt für Anorganische Chemie der Universität Göttingen, Göttingen, Germany, 1998. (b) Altomare, A.; Burla, M. C.; Camalli, M.; Cascarano, G. L.; Giacovazzo, C.; Guagliardi, A.; Moliterni, A. G. G.; Polidori, G.; Spagna, R. *J. Appl. Crystallogr.* **1999**, *32*, 115–119.
(32) Holleman, A. F.; Wiberg, E.; Wiberg N. *Lehrbuch der Anorganischen Chemie*; Walter de Gruyter: Berlin, 1995.
(33) http://academic.pg.cc.md.us/~ssinex/struc_bond/oxides_of_nitrogen.htm.
(34) Klapötke, T. M.; Mayer, P.; Schulz, A.; Weigand, J. J. *J. Am. Chem. Soc.* **2005**, *227* (7), 2032–2033.

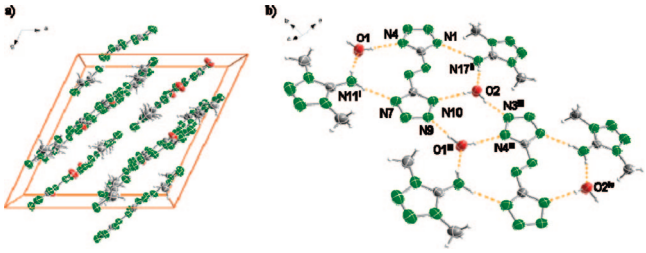

Figure 7. (a) View of the unit cell along the *b* axis and (b) hydrogen bonding in a layer in the crystal structure of azotetrazolate **1** (symmetry codes: (i) $x, -0.5 - y, 0.5 + z$; (ii) $x, -0.5 - y, -0.5 + z$; (iii) $x, -1 + y, z$; (iv) $x, -1 + y, z$).

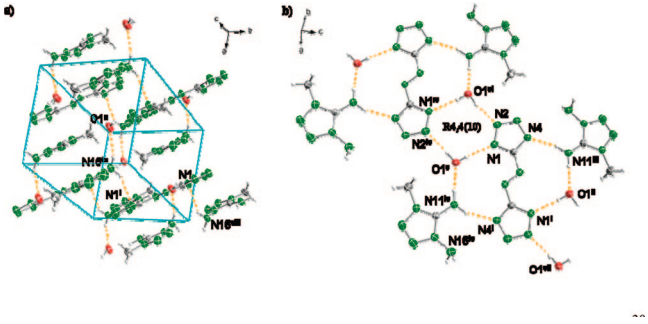

Figure 8. (a) Hydrogen bonding between layers and (b) in a layer in the crystal structure of azotetrazolate **3** (symmetry codes: (i) $2 - x, -y, 1 - z$; (ii) $2 - x, 1 - y, 1 - z$; (iii) $1 + x, y, 1 + z$; (iv) $1 - x, -y, -z$; (v) $x, -1 + y, z$; (vi) $1 - x, 1 - y, 1 - z$; (vii) $1 + x, y, 2 + z$; (viii) $1 - x, 1 - y, -z$; (ix) $1 + x, -1 + y, 1 + z$; (x) $x, -1 + y, 1 + z$).

groups form hydrogen bonds to N1^{i} and N7^{ii} of the azotetrazolate anion with distances of 2.889(4) and 2.876(4) Å, respectively (symmetry codes: (i) $x, -0.5- y, 0.5 + z$; (ii) $x, -0.5 - y, -0.5 + z$). There are no appreciable contacts between layers, the closest distance is between O2 and N19^{vi} at 3.902(4) Å (symmetry code: (vi) $x, 1.5 - y, 0.5 + z$). Description of the hydrogen-bonding networks is facilitated by the use of graph-set analysis as reported by Berstein et al. (unitary = primary = first order, binary = secondary = second order . . .).[35] The computer program *RPLUTO*[36–38] was used to identify unitary and binary graph-sets. The unitary hydrogen-bonding network (N_1) for **1** is made up of eight dimmeric interactions of the type **D1,1(2)**, which connect the anions and the cations, either directly or by means of bridging water molecules, forming a complex hydrogen-bonded structure. At the secondary level, the primary **D1,1(2)** dimeric interactions combine to form many **D2,2(4)** and **D2,2(9)** graph-sets and the less common **D2,2(5)** and **D2,2(8)** motifs, which extend, for example, from one of the hydrogen atoms on N11^{i} to one on O2, and from one of the hydrogen atoms on O2 to one on O1, respectively (symmetry code: (i) $x, -0.5 - y, 0.5 + z$). Two chain motifs defined as ***C*2,2(10)** including the two hydrogen atoms on O1 or O2 and the azotetrazolate azo-bridge to N9 or N3, respectively, are observed.

(35) Bernstein, J.; Davis, R. E.; Shimoni, L.; Chang, N.-L. *Angew. Chem., Int. Ed.* **1995**, *34* (15), 1555–1573.
(36) Motherwell, W. D. S.; Shields, G. P.; Allen, F. H. *Acta Crystallogr., Sect. B* **2000**, *56* (3), 466–473.
(37) Motherwell, W. D. S.; Shields, G. P.; Allen, F. H. *Acta Crystallogr., Sect. B* **1999**, *55* (6), 1044–1056.
(38) http://www.ccdc.cam.ac.uk/support/documentation/rpluto/TOC.html.

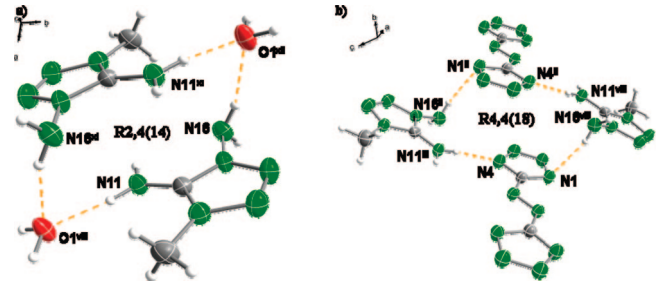

Figure 9. View of (a) **R2,4(14)** and (b) **R4,4(18)** hydrogen-bonding graph-sets in the crystal structure of azotetrazolate **3** (symmetry codes: (ii) $2 - x, 1 - y, 1 - z$; (iii) $1 + x, y, 1 + z$; (viii) $1 - x, 1 - y, -z$; (xi) $-x, 1 - y, -z$; (xii) $-1 + x, y, -z$).

In **3**, the inversion center of the space group (*P*-1) causes both halves of the azotetrazolate anion to be identical (Figure 6). The anions form four hydrogen bonds to two different water molecules with distances of 2.806(1) and 2.832(1) Å (Figure 8b). N3 and the azo nitrogen N5 do not form any significant hydrogen bond, whereas N4 forms a hydrogen bond to the C-bound amino group of the tetrazolium cations with N11−H11A···N4^{xiii} = 2.892(2) Å (symmetry code: (xiii) $-1 + x, y, -1 + z$). Both tetrazolium cations are also identical due to symmetry. The two cation amino groups have different hybridizations. The C-NH_2 is sp-hybridized whereas the N−NH_2 is sp-hybridized with the nitrogen lone pair directed toward the C−NH_2 nitrogen atom, yielding an intramolecular hydrogen bond (N11−H11A···N16 = 2.912(1) Å). It is this twisted sp^3-hybridized amino group that allows for the formation of hydrogen bonds with one of the anion nitrogen atoms of one layer (N16−H16B···N1^{viii} = 3.168(1) Å; symmetry code: (viii) $1 - x, 1 - y, -z$) and a water molecule of another layer (N16−H16A···O1^{xv} = 3.024(1) Å; symmetry code: (xv) $-1 + x, y, z$) as shown in Figure 8a. Using graph-set nomenclature, the primary graph-set for **3** is described by six **D1,1(2)** dimmeric interactions and an intramolecular hydrogen bond between N11 and N16, which takes the label **S(5)**. In analogy to **1**, multiple combinations of hydrogen bonds to form **D2,2(4)** and **D2,2(9)** secondary motifs are possible. Once again, the dimmeric **D2,2(5)** (e.g., from N11^{iv} to O1^{vii}, symmetry codes: (iv) $1 - x, -y, -z$; (vii) $1 + x, y, 2 + z$) and **D2,2(8)** (e.g., from one hydrogen atom on O1^{ii} to one on O1^{v}, symmetry codes: (ii) $2 - x, 1 - y, 1 - z$; (v) $x, -1 + y, z$) graph-sets as well as the ***C*2,2(10)** chain motif (from one hydrogen atom on O1^{vii} to N1) are found. Additionally, a longer ***C*2,2(12)** chain starting at N4 and finishing at one of the hydrogen atoms on N16^{iv} is observed. Further similarities in the hydrogen-bonding networks of **1** and **3** are observed. In the case of **3**, symmetry (symmetry code: (i) $2 - x, -y, 1 - z$) allows for the formation of a **R4,4(10)** ring motif at the secondary level, which is analogous to the ring hydrogen-bonded by N9, N10, O2, N3^{iii}, N4^{iii}, and O1^{iii} in the crystal structure of **1** (symmetry code: (iii) $x, -1+ y, z$), which involves four different hydrogen bonds and is thus generated at the quaternary level. Furthermore, the presence of the twisted N-bound amino group, allows for the formation of interlayer ring patterns of even higher order, namely **R2,4(14)** (Figure 9a) and **R4,4(18)** (Figure 9b), which are formed along two bridging water molecules or two azotetrazolate anions,

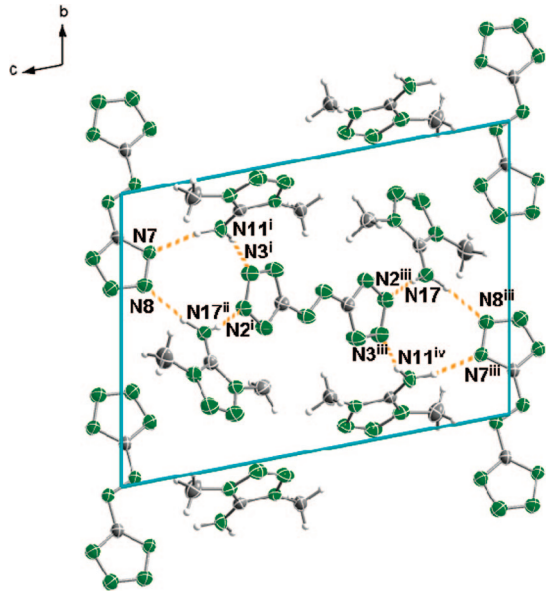

Figure 10. Hydrogen bonding around the azotetrazolate anion in the unit cell of azotetrazolate **2** (view along the *a* axis; symmetry codes: (i) $2 + x$, y, z; (ii) $3 - x$, $1 - y$, $1 - z$; (iii) $1 - x$, $1 - y$, $1 - z$; (iv) $2 - x$, $1 - y$, $1 - z$).

respectively. Lastly, this sp^3-hybridized amino group nitrogen atom ($N16^{v}$) forms one of the aforementioned hydrogen bonds between layers with N1, which in turn coordinates to one of the hydrogen atoms on $O1^{v}$ of a water molecule in the same layer, forming the relatively uncommon **D1,2(3)** pattern.

The absence of crystal water in compounds **2** and **4** results in nonlayered structures in contrast to the dihydrated species. In **2** (Figure 5), there are two types of azotetrazolate anions, which are symmetric and surrounded by four tetrazolium cations each one forming two different types of hydrogen bonds to the amino group hydrogen atoms (Figure 10). Both anions participate in different hydrogen bonding, whereas one of them coordinates face-on to two tetrazolium cations through hydrogen bonds (N11−H11A···N3 = 2.860(2) Å and N17−H17A···$N2^{iii}$ = 2.922(2) Å; symmetry code: (iii) $1 - x$, $1 - y$, $1 - z$), the other one interacts side-on (N11−H11B···N7 = 2.849(2) Å and N17−H17B···$N8^{iii}$ = 2.885(2) Å). The absence of crystal water in **2** reduces markedly the number of hydrogen atoms available to interact through dipole–dipole bonds and only half-as many hydrogen bonds as in the parent dihydrate **1** are formed (Table 7). The unitary graph-set is described by four **D1,1(2)** dimeric interactions. These combine at the secondary level to form further dimeric networks. For example, the usual **D2,2(4)** and **D2,2(9)** graph-sets can be found. Two **D2,2(5)** patterns in which $N11^{i}$ and $N17^{ii}$ of two cations link two azotetrazolate anions (symmetry codes: (i) $2 + x$, y, z; (ii) $3 - x$, $1 - y$, $1 - z$) and the usual **D2,2(8)** pattern described above for **1** and **3** are observed. Both **D2,2(5)** secondary graph-sets combine to form a pseudoring network with the nomenclature **R4,4(10)** (similar to **1**), starting at N7 and finishing at N8 (the pseudoring term refers to the fact that two secondary networks combine to form a quaternary one, when generally the graph-set analysis is limited to the secondary level). As described for **3**, the formation of this

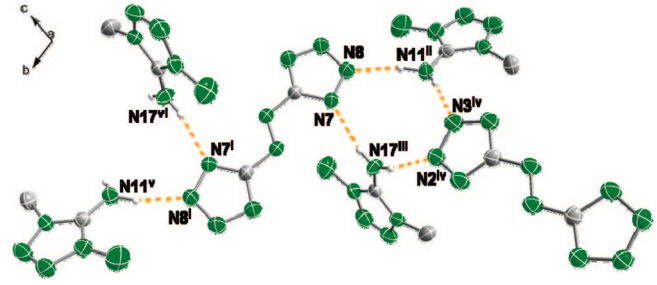

Figure 11. Hydrogen bonding around the anion in the crystal structure of azotetrazolate **4** (the hydrogen atoms on the disordered amino and methyl groups have been omitted for simplicity sake; symmetry codes: (i) $-x + 1$, $-y - 1$, $-z + 1$; (ii) $-x$, $-1 - y$, $-z$; (iii) $-x$, $-y$, $-z$; (iv) $-1 - x$, $-1 - y$, $-z$; (v) $-1 + x$, $2 + y$, $-1 + z$; (vi) $-1 + x$, $1 + y$, $1 + z$).

ring-pattern at the quaternary level is due to symmetry reasons. Lastly, four dimmer graph-sets **D2,2(10)** are formed (e.g., starting at one hydrogen atom on N17 and finishing on a hydrogen atom linked to $N17^{ii}$).

In **4**, the most significant changes in the cation distances are observed in the N−NH_2 and the N−CH_3 bond lengths (Table 5). Although in **3**, there is a noticeable difference between the N−NH_2 (1.383(1) Å) and N−CH_3 (1.455(1) Å) distances, in **4**, the bond distances are the result of averaged methyl and amino group positions and are thus very similar (1.449(3) and 1.455(3) Å). Further analysis of the disorder found in azotetrazolate salt **4** is out of the scope of this paper and will be omitted.

The disorder does not allow a complete analysis of the hydrogen-bonding situation in **4**. In Figure 11, the hydrogen bonding around the anion is depicted. Every anion is surrounded by four cations with which they interact via hydrogen bonding. Half of the anion is related to the other half by symmetry and forms one hydrogen bond to each one of the two crystallographically independent cations (N11−H11A···$N3^{vii}$ = 2.929(3) Å and N17−H17A···$N2^{vii}$ = 2.863(3) Å; symmetry code: (vii) $1 + x$, y, z), which, in turn, coordinate to the other crystallographically independent half of the anion (N11−H11B···$N8^{viii}$ = 2.884(3) Å and N17−H17B···$N7^{viii}$ = 2.852(3) Å; symmetry code: (viii) $1 - x$, $1 - y$, $1 - z$). Without taking into consideration the disordered methyl and amino groups, the hydrogen-bonding network is identical to that of **2**. Four primary dipole–dipole dimeric graph-sets **D1,1(2)** combine to form two **D2,2(4)**, two **D2,2(5)**, one**D2,2(8)**, one **D2,2(9)** and four **D2,2(10)** secondary motifs, exactly as observed for **2**. Lastly, once again, symmetry does not allow for the formation of a secondary graph-set **R4,4(10)**, but this is formed at the quaternary level instead.

Thermal and Energetic Properties. To assess the thermal and energetic properties of azotetrazolates **1–4** the thermal stability (decomposition points from DSC measurements), as well as the sensitivities to friction, impact, electrostatic discharge, and thermal shock of each salt were experimen-

(39) Impact: insensitive >40 J, less sensitive ≥35 J, sensitive ≥4 J, very sensitive ≤3 J; friction: insensitive >360 N, less sensitive = 360 N, sensitive <360 N a. >80 N, very sensitive ≤80 N, extreme sensitive ≤10 N. According to the UN Recommendations on the Transport of Dangerous Goods, (+) indicates not safe for transport.

Table 8. Initial Safety Testing Results and Predicted Energetic Performance of Nitrogen-Rich Azotetrazolate Salts 1–4 Using the EXPLO5 Code

	T_{ex} (K)[a]	V_0 (L kg^{-1})[b]	P_{det} (GPa)[c]	D (m s^{-1})[d]	impact (J)[e]	friction (N)[e]	ESD (+/−)[f]	thermal shock
1	2987	822	20.2	7820	>30	>360	−	deflagrates
2	3046	782	20.0	7803	>30	>360	−	explodes
3	2811	842	22.4	8090	>30	>360	−	explodes
4	3323	808	21.1	7977	>30	>360	−	explodes

[a] Temperature of the explosion gases. [b] Volume of the explosion gases. [c] Detonation pressure. [d] Detonation velocity. [e] Tests according to BAM methods (see refs 39−41). [f] Rough sensitivity to electrostatic discharge, + sensitive, − insensitive.

Table 9. Physiochemical Properties of Nitrogen-Rich Azotetrazolate Salts 1–4

	1	**2**	**3**	**4**
formula	$C_8H_{20}N_{20}O_2$	$C_8H_{16}N_{20}$	$C_6H_{18}N_{22}O_2$	$C_6H_{14}N_{22}$
mol. mass (g mol^{-1})	428.44	392.35	430.35	394.39
T_m (°C)[a]				
T_d (°C)[b]	197	193	183	170
ΔH_{sub} (kJ mol^{-1})[c]	88	88	86	83
N (%)[d]	65.4	71.4	71.6	78.1
Ω (%)[e]	−89.6	−97.8	−70.6	−77.1
ρ (g cm^3)[f]	1.441	1.431	1.546	1.427
ΔU_{comb} (cal g^{-1})[g,h]	−3800(30)	−4000(10)	−3000(10)	−3400(20)
$\Delta U°_f$ (kJ kg^{-1})[h,i]	+2800(100)	+3800(30)	+2200(40)	+4100(70)
$\Delta H°_f$ (kJ kg^{-1})[h,j]	+2700(100)	+3800(30)	+2200(40)	+4100(70)

[a] Chemical melting point from measurement with β = 5 °C min^{-1}. [b] Decomposition point (DSC onsets) from measurement with β = 5 °C min^{-1}. [c] Enthalphy of sublimation calculated according to ref 48. [d] Nitrogen percentage. [e] Oxygen balance according to ref 49. [f] Density from X-ray measurements. [g] Experimentally determined (oxygen bomb calorimetry) constant volume energy of combustion. [h] Uncertainty in parentheses. [i] Experimentally determined (back-calculated from ΔU_{comb}) energy of formation. [j] Experimentally determined enthalpy of formation.

Table 10. Thermodynamic and Explosive Properties of Formulations of Nitrogen-Rich Azotetrazolate Salts 1–4 with Ammonium Nitrate (AN)

	AN + 1[a]	AN + 2[b]	AN + 3[c]	AN + 4[d]
ρ (g cm^{-3})[e]	1.671	1.673	1.683	1.660
M (g mol^{-1})	142.69	133.09	157.07	146.01
Ω (%)[f]	+0.2	−0.1	+0.0	−0.4
$\Delta U°_f$ (kJ kg^{-1})[g]	−3132	−3019	−2964	−2631
$\Delta H°_f$ (kJ kg^{-1})[h]	−3266	−3148	−3100	−2767
T_{ex} (K)[i]	2987	3064	3010	3121
V_0 (L kg^{-1})[j]	953	949	953	949
P (GPa)[k]	24.5	24.6	24.7	24.5
D (m s^{-1})[l]	8034	8062	8063	8066

[a] 82% AN + 18% **1**. [b] 83% AN + 17% **2**. [c] 78% AN + 22% **3**. [d] 79% AN + 21% **4**. [e] Density from X-ray measurements. [f] Oxygen balance according to ref 48. [g] Calculated energy of formation. [h] Calculated enthalpy of formation. [i] Temperature of the explosion gases. [j] Volume of the explosion gases. [k] Detonation pressure. [l] Detonation velocity.

Table 11. Thermodynamic and Explosive Properties of Formulations of Nitrogen-Rich Azotetrazolate Salts 1–4 with Ammonium Dinitramide (ADN)

	ADN + 1[a]	ADN + 2[b]	ADN + 3[c]	ADN + 4[d]
ρ (g cm^{-3})[e]	1.727	1.729	1.737	1.713
M (g mol^{-1})	190.98	180.38	206.75	194.33
Ω (%)[f]	+0.4	−0.2	−0.2	+0.1
$\Delta U°_f$ (kJ kg^{-1})[g]	−242	−52	−196	+213
$\Delta H°_f$/kJ kg^{-1}[h]	−372	−183	−334	+77
T_{ex}/ (K)[i]	4000	4057	3960	4086
V_0 (L kg^{-1})[j]	890	885	894	886
P (GPa)[k]	31.1	31.3	31.6	30.9
D (m s^{-1})[l]	8792	8807	8761	8778

[a] 78% ADN + 22% **1**. [b] 79% ADN + 21% **2**. [c] 73% ADN + 27% **3**. [d] 75% ADN + 25% **4**. [e] Density from X-ray measurements. [f] Oxygen balance according to ref 48. [g] Calculated energy of formation. [h] Calculated enthalpy of formation. [i] Temperature of the explosion gases. [j] Volume of the explosion gases. [k] Detonation pressure. [l] Detonation velocity.

tally assessed (Tables 8 and 9) using standard BAM tests.[39–41] In addition, for all four CHN(O) salts, the constant volume energies of combustion (ΔU_{comb}) were determined experimentally using oxygen bomb calorimetry. The heats and energies of formation were back-calculated from the combustion data and subsequently used in conjunction with the molecular formula and density (from X-ray) to predict the detonation performance parameters (pressure and velocity) for each compound using the EXPLO5 computer code.[42] The detonation parameters for azotetrazolate salts **1**−**4** and formulations with an oxidant such as ammonium nitrate (AN) or ammonium dinitramide (ADN) were also calculated using the EXPLO 5 code and are tabulated in Tables 10 and 11. The formulations calculated were composed of compound and oxidant in oxygen neutral ratios. Table 12 shows a comparison of the detonation velocities and pressures of salts **1–4** with TNT, RDX, and the corresponding formulations with ADN.

Slow heating in a DSC apparatus (β = 5 °C min^{-1}) of samples of ∼1 mg of each energetic material gives rapid decomposition without melting at temperatures around 195 °C for compounds **1**and **2** and around 175 °C for **3**and **4** (Figure 12). For compounds **1**and **3** in addition to the decomposition exotherm, the DSC curves show an endotherm at 84 and 92 °C, respectively, corresponding to the loss of two molecules of crystal water. These studies show the azotetrazolate salts presented here have a high thermal stability, which most likely can be attributed to the extensive hydrogen bonding observed in the crystal structures. In addition to DSC analysis, all compounds were tested by placing a small sample (∼0.5–1.0 mg) of compound in the flame. This resulted in an vigorous reaction (deflagration) in the case of **1** and explosion in the case of **2–4** (both TNT and RDX explode under similar conditions).

Data collected for friction, impact, and electrostatic discharge sensitivity are summarized in Table 8. The compounds in this study are significantly less sensitive to friction and impact than analogous salts containing the same

(40) http://www.bam.de.
(41) Klapötke, T. M.; Rienäcker, C. M. *Propellants, Explos., Pyrotech.* **2001**, *26*, 43.
(42) Suceska, M. *Propellants, Explos., Pyrotech.* **1991**, *16* (4), 197–202.

Table 12. Comparison of Physiochemical and Explosives Properties of Nitrogen-Rich Azotetrazolate Salts 1–4 with Common Explosives and Their Formulations with AN and ADN

	ρ (g cm^{-3})[a]	Ω (%)[b]	P (GPa)[c]	D (m s^{-1})[d]
1	1.441	−89.6	20.2	7820
2	1.431	−97.9	20.0	7803
3	1.546	−70.6	22.4	8090
4	1.427	−77.1	21.1	7977
TNT	1.654	−74.0	20.5	7171
RDX	1.800	−21.6	34.0	8885
ADN	1.808	+25.8	22.7	7650
ADN + **1**[e]	1.727	+0.4	31.1	8792
ADN + **2**[f]	1.729	−0.2	31.3	8807
ADN + **3**[g]	1.737	−0.2	31.6	8761
ADN + **4**[h]	1.713	+0.1	30.9	8778
ADN + TNT[i]	1.768	−0.1	31.7•	8739
ADN + RDX[j]	1.804	+0.2	34.9•	9091

[a] Density from X-ray measurements. [b] Oxygen balance according to ref 48. [c] Detonation pressure. [d] Detonation velocity. [e] 78% ADN + 22% **1**. [f] 79% ADN + 21% **2**. [g] 73% ADN + 27% **3**. [h] 75% ADN + 25% **4**. [i] 74% ADN + 26% **TNT**. [j] 46% ADN + 54% **RDX**.

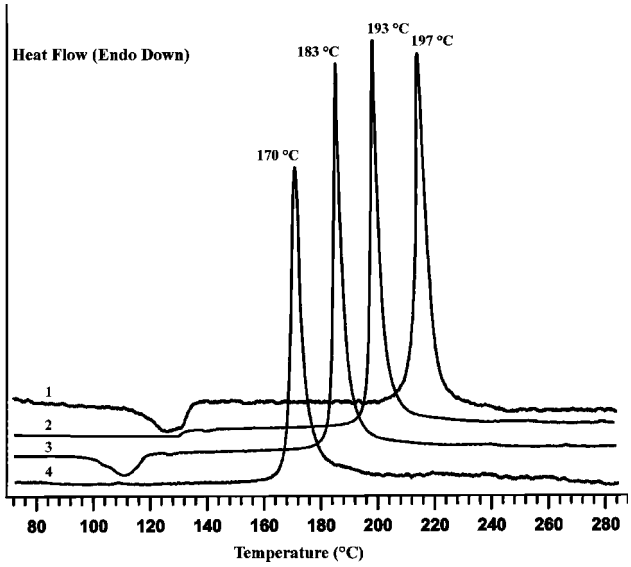

Figure 12. DSC plots for nitrogen-rich azotetrazolate salts **1**−**4** showing the loss of water (azotetrazolates **1** and **3**) and the decomposition temperatures at a heating rate of $\beta = 5$ °C min^{-1}.

cation.[22,27,34,43] None of the compounds showed sensitivity toward shock or friction. No detonation was observed in the drop hammer test (>30 J)[39–41] nor in the friction tester (>360 N). Also, no detonation occurred when grinding the compounds in a mortar. In addition, each compound was roughly tested for sensitivity to electrostatic discharge by spraying sparks across a small (a few crystals) sample of material using a tesla coil (ESD testing ~20 kV).

A comparison with the properties of TNT and RDX is useful to assess the energetic salts in this study. Salts **1**–**4** are much less sensitive to impact than TNT (15 J) and RDX (7.4 J).[44] This is to be expected because extensive hydrogen bonding helps to stabilize a material and interesting since the density and heat of formation (related to the performance) are favored by strong hydrogen bonds.[45] Hence, compounds that foreseeably form many hydrogen bonds are of interest as prospective insensitive materials with high performances.[46,47] All compounds under study were also less sensitive to friction and electrostatics than either TNT or RDX. Lastly, all materials reported here are safe for transport under the UN Recommendations on the Transport of Dangerous Goods.[39]

In addition to safety considerations, performance of new high-energy-density materials is of significant importance. Using the molecular formula, density (from X-ray), and energy of formation (ΔU_f), we can use the EXPLO5 computer code to calculate the detonation velocity and pressure of CHNO-based explosive materials. The following values for the empirical constants in the Becker−Kistiakowsky−Wilson equation of state (BKWN-EOS) were used: $\alpha = 0.5$, $\beta = 0.176$, $\kappa = 14.71$. and $\theta = 6620$. The detonation parameters for azotetrazolates **1**–**4** are presented in Table 8 and the experimentally determined energies of combustion and back-calculated energies of formation for compounds **1**−**4** are tabulated in Table 9 for sets of three individual measurements.

The physiochemical properties of all four compounds are tabulated in Table 9. Salts **1**–**4** have nitrogen contents between ~65 and 78% and highly negative oxygen balances (Ω) similar to TNT ($\Omega = -74.0\%$) between −71 and −98%. The densities, calculated from the X-ray measurements, are relatively low (~1.4 g cm^{-3}, except for **3**, for which $\rho > 1.5$ g cm^{-3}). The experimentally determined energies of combustion have values in the range from −3000(10) to ~−4000(10) cal g^{-1}. The energies of formation ($\Delta U°_f$) of salts **1**–**4** were back-calculated from the energies of combustion on the basis of their combustion equations, Hess's Law, the known standard heats of formation for water and carbon dioxide,[50] and a correction for change in gas volume during combustion. No corrections for the nonideal formation of nitric acid (typically ~5% of the nitrogen content reacts to form HNO_3) were made.

$$[C_3H_8N_5]^+{}_2[C_2N_{10}]^{2-} \times 2H_2O(s) + 12O_2 \rightarrow 8CO_2(g) + 10H_2O(l) + 10N_2(g)$$

$$[C_3H_8N_5]^+{}_2[C_2N_{10}]^{2-}(s) + 12O_2 \rightarrow 8CO_2(g) + 8H_2O(l) + 10N_2(g)$$

$$[C_2H_7N_6]^+{}_2[C_2N_{10}]^{2-} \times 2H_2O(s) + 9.5O_2 \rightarrow 6CO_2(g) + 9H_2O(l) + 11N_2(g)$$

$$[C_2H_7N_6]^+{}_2[C_2N_{10}]^{2-}(s) + 9.5O_2 \rightarrow 6CO_2(g) + 7H_2O(l) + 11N_2(g)$$

All $\Delta U°_f$ values are positive and higher in the case of the anhydrous species **2** and **4**, as expected. Exchange of a methyl group in **1** and **2** for an amino group in **3** and **4** would be expected to increase the energies of formation, however this is only observed in the case of the anhydrous species **4**.

(43) Kamlet, M. J.; Jacobs, S. J. *J. Chem. Phys.* **1968**, *48* (1), 23–35.
(44) Koehler, J.; Meyer, R. *Explosivstoffe*, 9th ed., Wiley-VCH: Weinheim, Germany, 1998.
(45) Cady, H. H.; Larson, A. C. *Acta Crystallogr.* **1965**, *18*, 485–496.
(46) Bemm, U.; Östmark, H. *Acta Crystallogr, Sect. C.* **1998**, *54*, 1997–1999.
(47) Westwell, M. S.; Searle, M. S.; Wales, D. J.; Williams, D. H. *J. Am. Chem. Soc.* **1995**, *117*, 5013–5015.
(50) Shimanouchi, T. *Tables of Molecular Vibrational Frequencies Consolidated*; National Bureau of Standards 1: Gaithersburg, MD, 1972; Vol I.

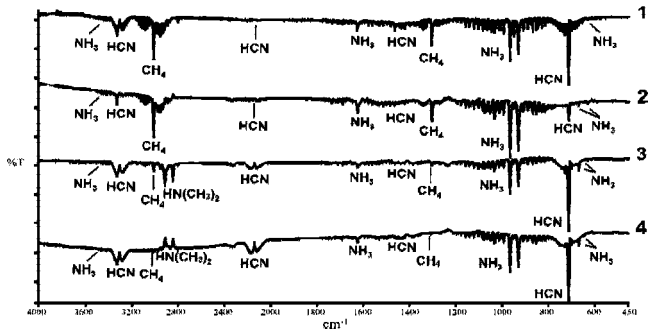

Figure 13. Infrared spectra of the decomposition products of nitrogen-rich azotetrazolate salts **1**−**4**.

3 has a low value of $\Delta U°_f = +2200(40)$ kJ kg^{-1}, which is, however, still higher than that of the 1,4,5-trimethyltetrazolium salt described in the literature.[18] The other dihydrated compound (**1**) has a higher (positive) value than **2**, whereas the anhydrous salts show considerably greater positive heats of formation comparable to bishydrazinium 5,5′-azotetrazolate for which $\Delta U°_f = +3700$ kJ kg^{-1}.

The azotetrazolate salts synthesized have detonation velocities (D) that vary within a narrow range and take values between 7800 and 8100 m s^{-1} (Table 8), higher than TNT ($D = 7171$ m s^{-1}) but lower than RDX ($D = 8885$ m s^{-1}). The detonation pressures (P) have values between 20.0 and 22.4 GPa and are comparable to that of TNT ($P = 20.5$ GPa). The greater values for the calculated detonation parameters of azotetrazolate **3** in comparison to **1**, **2**, and **4** can be attributed to the higher density of the same ($\rho = 1.546$ g cm^{-3} vs $\rho \sim 1.4$ g cm^{-3}). Mixtures of **1**−**4** with AN (Table 10) show, in general, only a slight increase in D (∼8060 m s^{-1}) and P (∼24.6 GPa), similar to TNT formulations with AN ($D = 8086$ m s^{-1} and $P = 25.4$·GPa), whereas mixtures with ADN (Table 11) have a much better predicted performance with $D \approx 8800$ m s^{-1} and $P \approx 31.0$ GPa, comparable to TNT + ADN and slightly less powerful than RDX + ADN (Table 12).

Decomposition Experiments. The mass spectra (EI$^+$) of the decomposition products of the nitrogen-rich salts **1**–**4** are, as expected, dominated by a peak with $m/z = 28$ corresponding to the formation of molecular nitrogen ($N_2^{\cdot+}$). In addition, the following fragments are formed: $m/z = 12$ (C^{4+}), 13 (CH^{3+}), 14 (CH_2^{2+}, N^+), 15 (CH_3^+), 16 ($CH_4^{\cdot+}$, NH_2^+), 17 ($NH_3^{\cdot+}$), 18 (CH_4) and 27 ($HCN^{\cdot+}$).[50–52] For **1** and **2**, a small additional peak at $m/z = 41$ with its corresponding fragmentations, which is assumed to be due to the formation of acetonitrile in the gas phase upon decomposition, is found. On the other hand, for **3** and **4**, dimethylamine ($m/z = 44$) forms instead of acetonitrile. The IR spectra of the decomposition gases of compounds **1**–**4** were measured (Figure 13). The formation of water and acetonitrile (liquid at room temperature) was not observed in the IR gas measurements due to the presence of these species in the condensed phase. The results are in accordance with the mass spectrometry measurements (Figure 14). Apart from molecular nitrogen, NH_3, HCN and CH_4 formed on

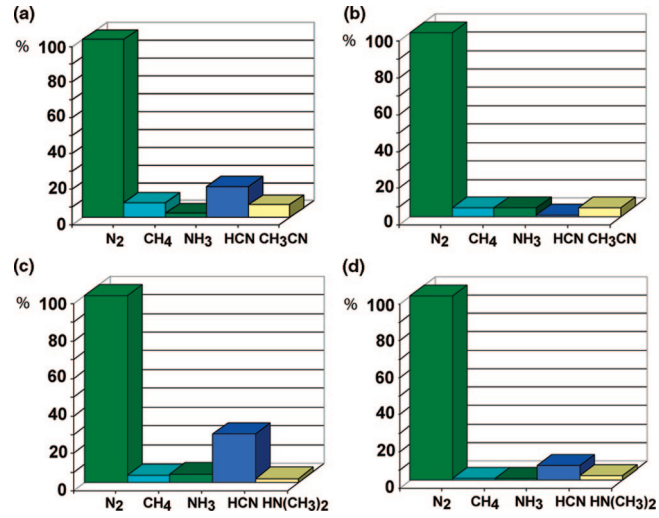

Figure 14. Experimental normalized molar percentage of decomposition gases as estimated by mass spectrometry for nitrogen-rich azotetrazolate salts (a) **1**, (b) **2**, (c) **3**, and (d) **4**. The amount of toxic HCN formed is expected to be highly overestimated in respect to the amount of N_2 because of the higher ease of ionization of HCN in respect to N_2.

decomposition (also CH_3CN for **1** and **2** and $HN(CH_3)_3$ for **3** and **4**). With the exception of compound **2**, HCN is formed as the second major gas product after N_2. In **3**, the amount of HCN formed is ∼1/3 of the amount of nitrogen gas formed. However, it must be kept in mind that HCN is much more easily ionized than N_2, and as a consequence the amounts of HCN, calculated from the intensities of the peaks in the EI$^+$ experiments, are expected to be highly overestimated. In addition, the predicted decomposition gases were calculated using the ICT code (Figure 15).[53] As expected, the major gas is molecular N_2 and the rest of the predicted gases are very similar in the case of salts **1** and **2** and salts **3** and **4**, with the main exception being the formation of water, not observed in the experimental measurements due to the presence of the same in the condensed phase. The replacement of a methyl group in **1** and **2** by an amino group in **3** and **4** is anticipated to produce higher amounts of NH_3 and lower amounts of CH_4, as observed experimentally, although ammonia forms in smaller amounts than expected. In addition, for compounds **1** and **3**, the program predicts the formation of minute amounts of CO and CO_2 not observed by neither MS nor IR experiments. This is probably due to the fact that the crystal water remains as such after combustion and does not react to oxidize the carbon atoms in the compounds. Relatively high molar amounts of H_2 would be expected from the calculation of the explosion gases for azotetrazolates **1**−**4**, however this could not be observed in the MS due to the low molecular mass of hydrogen, which falls out of the measuring range. According to the ICT code, only very small amounts of HCN form upon decomposition when in fact relatively large amounts could

(51) Shimanouchi, T. *J. Phys. Chem.* **1972**, *6* (3), 993–1012.
(52) Pretsch, E.; Bühlmann, P.; Affolter, C.; Herrera, A.; Martínez, R. *Determinación Estructural de Compuestos Orgánicos*; Springer-Verlag Ibérica: Barcelona, 2001.
(53) (a) *ICT-Thermodynamic Code, version 1.0*, Fraunhofer-Institut für Chemische Technologie (ICT): Pfinztal/Berghausen, Germany, 1988–2000. (b) Webb, R.; van Rooijen, M. *Proceedings of the 29th International Pyrotechnics Seminar*,Westminster, CO, July 14−19, 2002; International Pyrotechnics Society, 2002; pp 823–828. (c) Bathelt, H.; Volk, F. *27th International Annual Conference of ICT*, 1996, Vol. 92; pp 1–16.

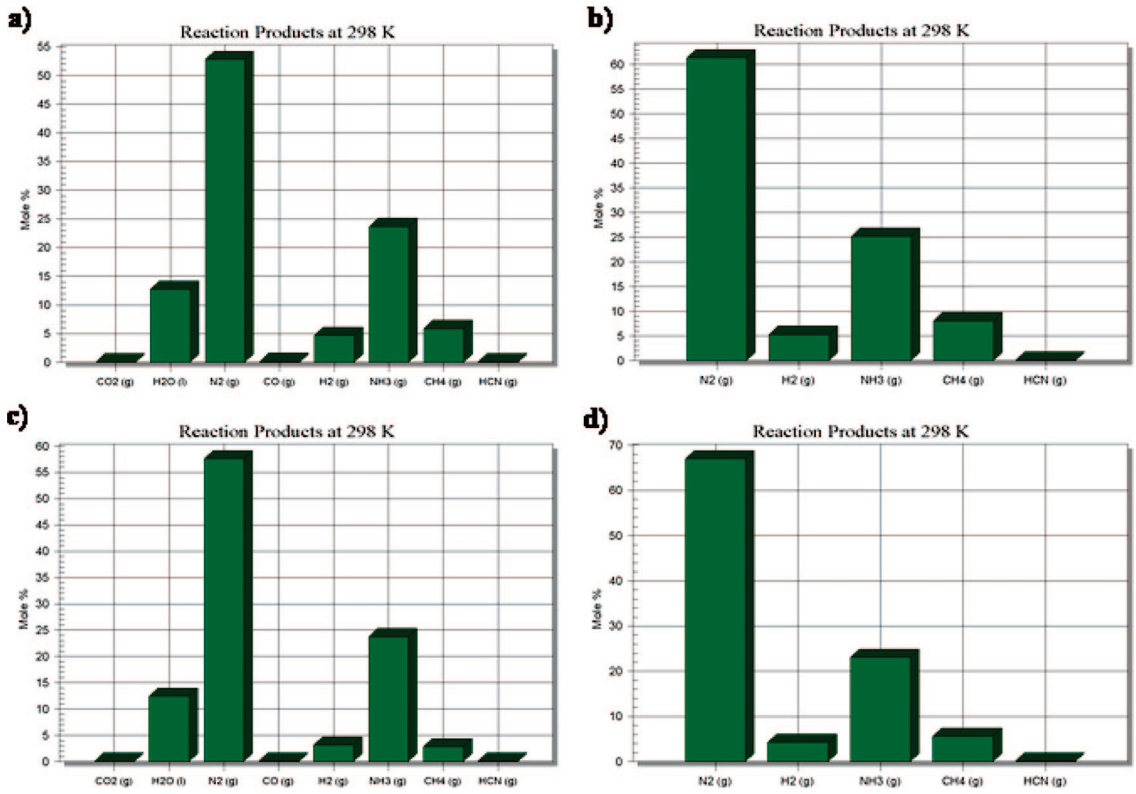

Figure 15. Predicted molar percentage of decomposition gases using the ICT code for nitrogen-rich azotetrazolate salts (a) **1**, (b) **2**, (c) **3**, and (d) **4**.

be detected by both IR and MS. Lastly, the formation of CH_3CN and $HN(CH_3)_2$ were not predicted by the code.

Conclusions

Convenient syntheses for nitrogen-rich tetrazolium azotetrazolate salts are reported. The new compounds were fully characterized by analytical and spectroscopic methods. In addition, their crystal structures in the solid state were determined by diffraction techniques. The hydrogen-bonding networks in compounds **1**−**4** are described in terms of graph-set analysis. All compounds turned out to be insensitive to shock, friction, and electrostatic discharge as determined by standard BAM tests and thermally stable to temperatures above 170 °C (DSC onsets). Lastly, bomb calorimetry measurements allowed the calculation of the detonation parameters (EXPLO5) of the new salts, revealing performances similar to that of TNT but with much more environmentally friendly explosion gases, as predicted by the ICT code.

Acknowledgment. Financial support of this work by the Ludwig-Maximilian University of Munich (LMU), the Fonds der Chemischen Industrie (FCI), the European Research Office (ERO) of the U.S. Army Research Laboratory (ARL) under Contracts N 62558-05-C-0027, W911NF-07-1-0569 and 9939-AN-01, and the Bundeswehr Research Institute for Materials, Explosives, Fuels and Lubricants (WIWEB) under Contracts E/E210/4D004/X5143 and E/E210/7D002/4F088 is gratefully acknowledged. The authors also thank Jan Welch for proofreading the manuscript.

CM703344H